Report #25-UT-171

NSTSCE

National Surface Transportation Safety Center for Excellence

Data-Driven Characterization of Motorcycle Riders' Kinematics and Crash Risk

Paolo Terranova, Robert McCall, Miguel A. Perez

Submitted: August 5, 2025

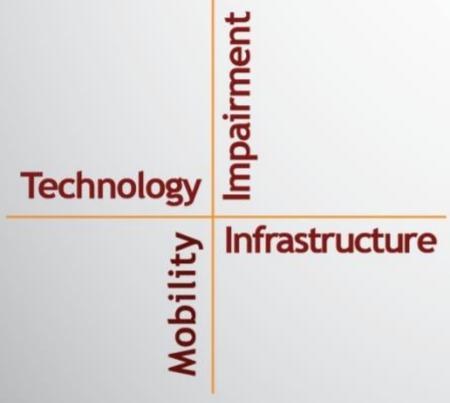

Housed at the Virginia Tech Transportation Institute
3500 Transportation Research Plaza • Blacksburg, Virginia 24061

ACKNOWLEDGMENTS

The authors of this report would like to acknowledge the support of the stakeholders of the National Surface Transportation Safety Center for Excellence (NSTSCE): Zac Doerzaph from the Virginia Tech Transportation Institute; John Capp and Yi Glaser from General Motors Corporation; Terri Hallquist and Jonathan Mueller from the Federal Motor Carrier Safety Administration; Mike Fontaine from the Virginia Department of Transportation and the Virginia Transportation Research Council; and Melissa Miles and Elizabeth Pulver from State Farm Insurance.

The NSTSCE stakeholders have jointly funded this research for the purpose of developing and disseminating advanced transportation safety techniques and innovations.

EXECUTIVE SUMMARY

This effort was successful in exploring different motorcycle riding styles using multiple, commonly available sensors, ultimately associating those results with potential crash events. More specifically, the analysis carried out in this work provides novel insights into real-world motorcyclist behavior by identifying three distinct riding profiles characterized by unique kinematic patterns. Furthermore, several potential kinematic indicators that may predict crash risk were identified. This enhanced characterization of motorcycle rider capabilities could enable more realistic crash-scenario simulations, inform evidence-based safety policies, and support the design of advanced rider-assistance systems that leverage real-world parameters.

In this study, riding styles and their relationship with crash and near-crash (CNC) risks were investigated using naturalistic riding study data from 155 participants over an average period of 11 months. The data, predominantly from southern California, includes approximately 400,000 miles of riding, providing extensive insight into real-world motorcycle riding behaviors.

The research addresses two main questions:

1. What defines the normal riding behavior of a motorcycle? Can it be categorized in terms of riding style?

2. What measures of rider performance are associated with crash risk?

Kinematic data collected from the instrumented motorcycles was processed to remove artifacts and noise prior to analysis. The analytical approach identified three distinct riding style clusters through principal component analysis and K-means clustering. The first cluster of 24 participants was primarily composed of younger participants using sport motorcycles. These subjects exhibited higher accelerations, abrupt braking, and substantially higher roll angles more frequently than other clusters. Additionally, this group showed significantly higher CNC rates than other clustered riders. Cluster 2 exhibited typical riding behavior, with moderate acceleration, braking, and roll rate values across a mix of motorcycle types and rider ages. In contrast, the riding behavior of the third cluster was smoother, with less aggressive maneuvers and safer distances during car-following scenarios. This third cluster was mainly composed of older participants primarily riding cruiser motorcycles. Statistical analysis revealed that age and motorcycle type significantly differentiated these clusters, whereas gender, riding experience, and formal training had minimal impact.

A bootstrap analysis comparing CNC trips against trips without a CNC (i.e., baseline trips) identified abrupt initial jerk during braking and accelerating maneuvers as a significant indicator of elevated crash risk, underlining the critical role of anticipatory and reactive behaviors in rider safety.

These findings offer critical insights for targeted rider education, motorcycle design, safety policy formation, and evaluation and design of advanced rider assistance systems. This enhanced understanding of motorcycle kinematic metrics and their linkage with crash risk can also inform insurers as they develop more precise, data-driven telematics-based rate structures.

TABLE OF CONTENTS

LIST OF FIGURES

LIST OF TABLES

LIST OF ABBREVIATIONS AND SYMBOLS

U.S.	United States
NHTSA	National Highway Traffic Safety Administration
NDS	naturalistic driving study
NRS	naturalistic riding study
IMU	inertial measurement unit
MSF	Motorcycle Safety Foundation
VTTI	Virginia Tech Transportation Institute
CNC	crash/near-crash
ANOVA	analysis of variance
ADAS	Advanced Driver Assistance Systems
ARAS	Advanced Rider Assistance Systems
ADS	Advanced Driving System
MVMT	million vehicle miles traveled

CHAPTER 1. INTRODUCTION AND BACKGROUND

The current effort intends to characterize normal and abnormal motorcycle riding styles and to predict crash and near-crash (CNC) risk by analyzing kinematic data. This work is timely due to both advances in telematics and kinematic data collection technologies, and the recent dramatic trends in motorcycle fatal crash statistics.

In 2024, the United States (U.S.) experienced roughly 6 million road crashes, resulting in 39,221 fatalities (National Highway Traffic Safety Administration [NHTSA], 2024b). Fatalities involving occupants of cars and light trucks accounted for 30% of the total, while motorcyclists contributed 15%—a disproportional result given that motorcycles represent only the 3% of the total nation's registered vehicles (NHTSA, 2019; NTSHA, 2024). Moreover, when analyzed as fatalities per vehicle miles traveled, the disparity becomes even more evident: motorcycles have a fatality rate of 26.2 compared to just 1.2 for passenger cars, indicating motorcyclists are nearly 22 times more likely than passenger car occupants to be killed in a crash per mile traveled (NHTSA, 2024a; Stewart, 2023). This disproportionate risk underscores the urgent need for targeted research and intervention strategies to reduce motorcycle-related fatalities in the U.S.

To address this risk and develop new motorcycle-specific crash countermeasures, a deeper understanding of motorcyclists' riding behaviors is essential. Comprehensive analyses of motorcycle–car collisions have repeatedly identified human factors as primary crash contributors (Huertas-Leyva et al., 2021; Penumaka et al., 2014; Sarkar et al., 2023). Nevertheless, existing studies on motorcycle crash risk often rely on questionnaire-based surveys (Sakashita et al., 2014) or retrospective crash analyses (Puthan et al., 2021; Terranova et al., 2023, 2025), both of which provide limited data for rider behavior analyses. While surveys yield important insights into social and psychological influences that could be used to inform new policies, they lack the precision to capture on-road rider behavior. Crash analyses are beneficial for estimating injury outcomes and identifying contributory factors, but they offer limited perspectives on real-time rider behavior and decision-making processes.

Another substantial portion of existing motorcycle research relies on controlled test-track experiments and simulator studies. These approaches provide controlled conditions for examining braking, lean/roll angles, and other kinematic metrics and can provide some insight into more real-time applications (Crundall et al., 2013; Davoodi et al., 2012; Davoodi & Hamid, 2013; Dunn et al., 2012; Huertas-Leyva et al., 2019; Kovácsová et al., 2020; Nugent et al., 2019; Yuen et al., 2014). However, these types of study also have inherent limitations, such as deviations from normal riding behavior. In addition, simulators often struggle to replicate real-world conditions (Boer et al., 2001; Jamson & Smith, 2003). While simulators are useful for qualitatively assessing riders' capabilities in specific contexts (e.g., emergency braking) or comparing experience levels, they cannot provide the level of detail and accuracy needed to characterize on-road behaviors in everyday traffic.

In contrast, real-world driving kinematics analyses, such as naturalistic research or telematics data, can provide a real-time perspective of how human actions contribute to collision risk and enable a comprehensive characterization of driver behavior (Ali et al., 2021, 2023; Dingus et al., 2016; Perez et al., 2024; Valente et al., 2024). Specifically, naturalistic driving studies (NDSs) are longitudinal efforts that collect extensive, uninstructed driving data over extended periods.

NDSs equip participant vehicles with data recording instruments (i.e., data acquisition systems, or DASs) and record every trip taken. Data collection tools range from GPS sensors to entire sensor-suites consisting of cameras, radars, inertial measurement units (IMUs), manufacturer data via the vehicle network, as well as in-vehicle monitoring systems (Dingus et al., 2016; Jain & Perez, 2025; Valente et al., 2023).

NDSs can vary in the ways that they collect data. For instance, some use a single equipped vehicle and multiple drivers, each with a relatively short period of participation (e.g., 3 months). Other, typically larger, efforts equip multiple vehicles that belong to individual participants for extended periods of time. Because NDSs often involve large sample sizes and continuous real-world observation that accumulate large quantities of data, they are particularly valuable for developing population-wide distributions of driver behaviors and capabilities.

Motorcycles, however, present unique challenges when conducting an NDS. First, with the lack of a readily available enclosed structure, the DAS must be protected from extreme heat, moisture, and cold in some other manner. Second, many motorcycles lack an accessible vehicle network, so all data collection equipment must be external. Third, equipment must be designed to survive in the event of a severe crash without the benefits afforded to larger vehicles for crash mitigation. These drawbacks, along with the large expense of NDSs in terms of instrumentation and data storage, have resulted in only a limited number of motorcycle-focused NDSs. Several such attempts are worthy of additional discussion.

Researchers at the Université Paris-Est, specifically, have been leading contributors in the collection of naturalistic riding studies (NRS) in Europe, primarily targeting novice motorcyclists over relatively short data-collection periods (Espié et al., 2013). For example, the SIM2Co+ project collected over 15,000 km of video and kinematic data from eight participants over 2 months to identify high-risk situations for newly licensed riders (Espié et al., 2013). In a separate study, 14 trainees were monitored for 5 months, yielding approximately 342 hours of data (Aupetit et al., 2013). The same research group coordinated the CSC-2RM project, which investigated commuting habits in the Paris region and recorded 85 hours of data from eleven riders and two motorcycles over 1 month (Espié et al., 2013). Finally, a separate investigation followed six novice riders over more than 2 months, documenting every trip they made, collecting 14,000 km worth of data (Aupetit et al., 2016). These studies have successfully demonstrated the feasibility of naturalistic motorcycle research and provided valuable insights into the behavior of novice riders; however, they were not designed to capture the full range of motorcycle riders' kinematic capabilities.

Similarly, the European "2-BE-SAFE – 2-Wheeler Behavior and Safety" initiative conducted a series of small-scale NRSs aiming to explore risky rider behaviors (Weare et al., 2011). The data collected was used by Vlahogianni et al. (2011, 2014) to propose a methodology to identify riding profiles and detect irregular behavior. Their approach relied on data gathered over a 3-month period from a single rider who regularly traveled the same route for 20-minute trips. By employing a distance-based outlier algorithm, the authors were able to recognize instances where the rider's behavior deviated significantly from their established norms. While the method effectively highlighted departures from the rider's established norms, the absence of actual CNC events prevented any correlation between atypical riding behaviors and increased crash risk. Baldanzini et al. (2016) faced a similar limitation when characterizing the braking styles of five

riders using one instrumented scooter over 2 months. Although they cataloged 3,573 braking events and offered an initial breakdown of real-world braking approaches, their goal was to explore the different braking approaches within the same rider. Additionally, they could not link the different approaches to specific CNC outcomes, missing a correlation between behaviors and risk. Moreover, small sample sizes, limited geographic regions, and a narrow set of instrumented vehicles further reduced the broader applicability of these findings. Nonetheless, these initial efforts were pivotal in guiding the design of future large-scale data collection projects, offering valuable insights into methodological challenges and providing a basis for more robust NRSs.

This evolution is evident in recent studies from Asia. For instance, a pilot NRS in Malaysia demonstrated that low-cost data collection methods are feasible, although the study involved only a small cohort of participants (Ibrahim et al., 2019). Akinapalli et al. (2023) tracked a much larger cohort of 58 riders in India along a predetermined 32 km round-trip route, successfully blending experimental and observational approaches to capture a comprehensive set of data.

In the U.S., in 2011, the Motorcycle Safety Foundation (MSF) and the Virginia Tech Transportation Institute (VTTI) launched the world's first large-scale NRS: the MSF100 Motorcyclists Naturalistic Study. The 100 recruited participants rode their own motorcycles for approximately 38,581 trips, corresponding to a total of 9,478 hours and 363,000 miles of riding over 40 different U.S. states. This data provided several important insights, such as information about the riders' usage of protective gear (V. Williams et al., 2013), the usage patterns of motorcycles (McCall et al., 2014), and the reliability of riders' self-reported mileage versus the actual riding mileage (V. Williams et al., 2017). Additionally, with more than 150 CNCs in the dataset (see Williams et al. [2016] for event categorization), this data provided important insights on the influence of several factors (e.g., aggressive riding style and lack of knowledge/skill; Williams et al., [2015]) as incrementors of motorcycle crash risk. Subsequent kinematic analyses of the MSF100 data examined speed metrics by participant sex and motorcycle type (Rainey et al., 2014) as well as acceleration patterns and their relationship with riders' experience (Rainey et al., 2021; Rainey & McLaughlin, 2017). Hard deceleration events during emergencies were also compared with those in passenger vehicles to identify potential similarities (V. Williams et al., 2018).

Although these studies have significantly advanced the understanding of rider capabilities, the specific kinematic differences among riders—and how these differences correlate with crash risk—remain largely unexplored. In today's era of advanced data analytics, developing a comprehensive and detailed parametrization of rider behavior is increasingly important. This is particularly critical given that driver and rider telematics are now widely employed for predictive crash analysis by stakeholders such as data brokers, insurance companies, and vehicle technology manufacturers. Given these needs, the research questions considered in this study were:

- What defines the normal riding behavior of a motorcycle? Can it be categorized in terms of riding style?

- What measures of rider performance are associated with crash risk?

CHAPTER 2. METHODS

DATASET OVERVIEW

The data employed from this analysis was obtained from one of the largest NRS databases in the world, housed at VTTI and comprised of data from 155 participants (McCall et al., in press; V Williams et al., in press). Motorcycles in the study were instrumented to collect kinematic data, video of riders and surroundings, and, for a subset of riders, frontal radar readings. Data collection spanned an average of 11 months per participant (ranging from 1.6 to 18 months) and occurred primarily in southern California, although riders also traveled in several other states. The participant group included 139 men and 16 women with an average age of 46 years (±14), ranging from 20 to 82 years.

In total, 101 CNC events were recorded (23 crashes and 78 near-crashes), involving 58 riders who each experienced between one and five events. The instrumented motorcycles used in the study could be categorized as either: (1) cruisers (n = 74), characterized by a low seat height, relaxed riding posture, and forward-set footpegs; (2) sport bikes (n = 77), known for their aggressive riding position, lightweight design, and aerodynamic fairings; and (3) touring bikes (n = 4), which feature a larger frame, upright seating, full fairings, and are often equipped with saddlebags for long-distance travel. Preliminary questionnaire data showed that 131 riders self-reported as experienced, 19 as novice, and 5 as returning riders (i.e., returning to riding for less than 1 year after a break of 5 years or longer). All 155 riders reported some level of formal rider training (42 reported low-level training, 109 reported having medium-level training, and 4 reported high-level training).

The database contains approximately 400,000 miles of riding data, covering over 51,000 trips and totaling 13,000 hours of ride time. On average, each participant recorded 2,555 miles, with individual totals ranging from 51 to 15,000 miles. Riders over 50 years old contributed 43% of the overall mileage and were responsible for roughly 70% of the miles travelled by cruiser motorcycles (Figure 1).

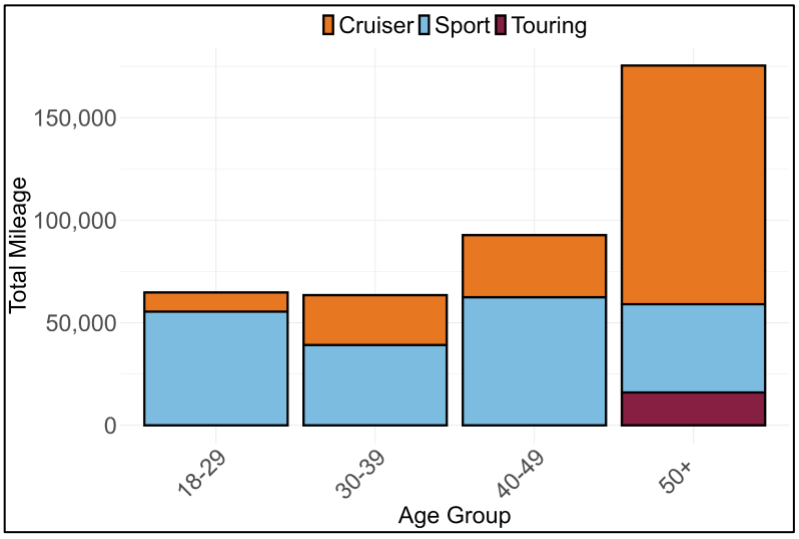

Figure 1. Graph. Total mileage by motorcycle type and age group.

In terms of road categories, about 40% of the total miles were travelled on roads classified as Level 1 and 2, defined as "*roads allowing for high volume, maximum speed traffic movement between and through major metropolitan areas*" (HERE Maps XML, 2025). Similarly, roads with speed limits between 60 and 65 accounted for about 40% of the total miles available in the database (Figure 2).

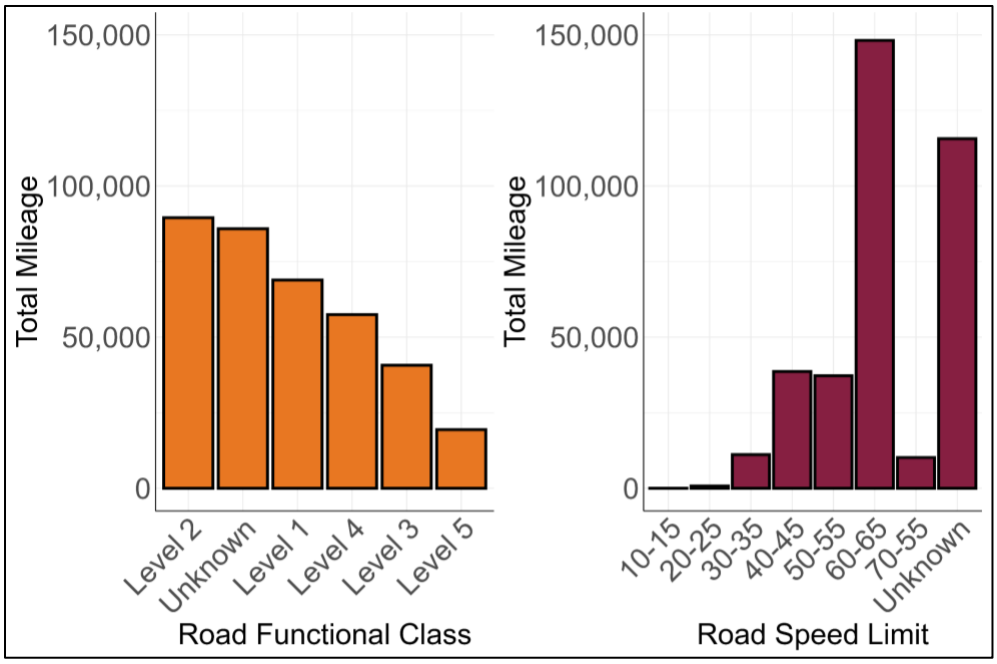

Figure 2. Graphs. Total mileage by road type classifications and speed limits.

DATA PROCESSING

This study built upon the approach proposed by Ali (2023) and Ali et al. (2021, 2023) for car-based NDS analyses, implementing new procedures to accommodate motorcycle-specific characteristics. Raw IMU-derived kinematic data was extracted and adjusted to account for the motorcycle's lean angle, and different signal processing approaches were tested to minimize noise introduced by vibration. The final methodology applied a seventh-order Butterworth low-pass filter to mitigate high-frequency noise. To eliminate vibration-caused biases in low-dynamics conditions, the kinematic data was set equal to zero whenever its moving standard deviation was lower than 0.2 and the vehicle speed dropped below 1 mph (Figure 3).

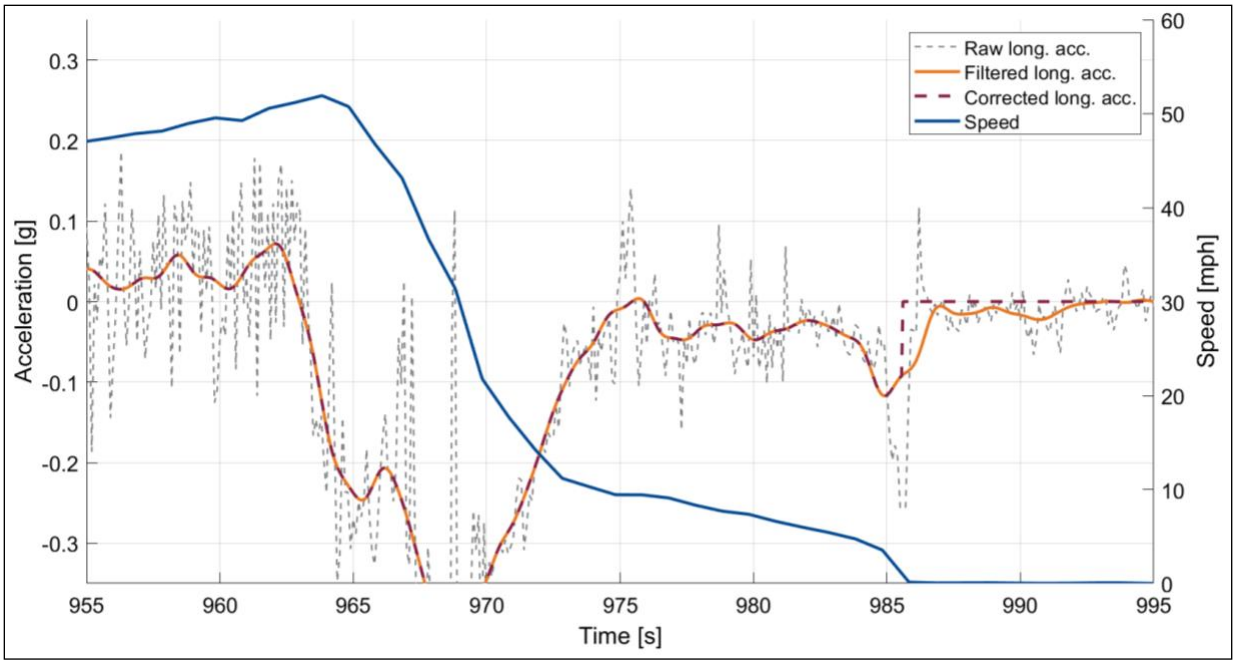

Figure 3. Graph. Example of the signal processing approach employed.

When available, radar data was extracted and processed to determine the spatial and temporal separations between the ego-motorcycle and the vehicles ahead. Car-following scenarios were isolated by excluding targets not labeled as a leading vehicle by the radar unit's onboard logic. GPS data was paired with digital maps to incorporate speed limits and road types, while brake signal information was captured from the vehicle's electrical system.

APPROACH

Motorcycle rider behavior was captured through the analysis of two important metrics in motorcycle dynamics: the longitudinal acceleration and the roll rate. High longitudinal deceleration shortens reaction time, while high positive values can affect the motorcycle's stability (Deligianni et al., 2017; Limebeer et al., 2001; Tak et al., 2015). Roll rate—the speed at which a rider leans—differentiates aggressive, tight turns from smoother trajectories and has proven useful in unsupervised skill assessment and rider clustering (Bartolozzi et al., 2023; Diop et al., 2023; Magiera et al., 2016).

These metrics were analyzed through an epoch-based algorithm, where the "epochs" were defined as any continuous interval during which the acceleration or roll rate surpassed predetermined thresholds. Figure 4 shows this concept applied to longitudinal acceleration, illustrating defined acceleration and deceleration epochs distinguished from baseline fluctuations. Different threshold values were tested to achieve a balance between removing noise and capturing significant epochs, ultimately adopting ±0.01g for longitudinal acceleration and ±1 deg/s for roll rate.

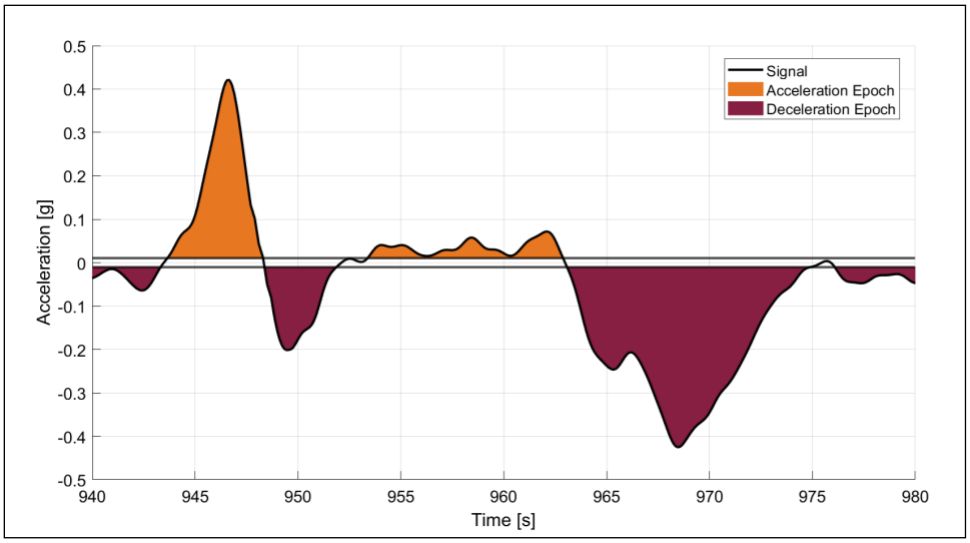

Figure 4. Graph. Epoch-based algorithm – example applied to longitudinal acceleration.

A comprehensive set of metrics was computed for each epoch identified through this methodology and used to characterize both the riding environment and rider behavior (Table 1). Metrics were chosen to capture detailed trip-level attributes (e.g., speed, distance traveled, road type, and curvature) as well as precise dynamics features within each epoch (e.g., peak, mean, and median values of acceleration or roll rate, jerk, and roll angle). For epochs associated with longitudinal acceleration, additional metrics—including acceleration percentiles, longitudinal jerk statistics, and comparisons between IMU and GPS measurements—were additionally gathered to precisely assess rider behavior during acceleration and braking events. Similarly, for roll rate epochs, metrics related to roll angle percentiles, peak roll rates, and the temporal distribution of roll dynamics within the epoch were employed to characterize cornering style, rider aggressiveness, and smoothness during turns.

Table 1. List of metrics extracted for each longitudinal acceleration and roll rate epoch.

Metric name	Meaning and unit of measure
FILE_ID	Trip identification number
PARTICIPANT_ID	Participant identification number
DISTANCE	Distance travelled in the epoch [m]
DURATION	Duration of the epoch [ms]
TIME_START/END	Time start and end of the epoch [ms]
TIME_PEAK_EPOCH	Time of the metric peak as % of the epoch length [%]
SPEED_START/END	Speed at start and end epoch [mph]
SPEED_CHANGE	Speed difference in epoch [mph]
SPEED_MAX/MIN	Speed max and min in epoch [mph]
SPEED_AT_PEAK	Speed at peak of the metric [mph]
CURVE	Presence of a curve
RADIUS	Radius of curvature
BRAKING_INT	Brakes activated in the epoch
BRAKING_1SEC	Brakes activated in 1 sec. interval around the epoch
SPEED_LIMIT	Speed limit of the road [mph]
ROAD_CLASS	Road type classification

Metric name	Meaning and unit of measure
Specific metrics for longitudinal acceleration epochs [POS = acceleration; NEG = deceleration]	
POS/NEG_ACC_PEAK/MEAN/MEDIAN_IMU	Long. acc. peak, mean, median from IMU [g]
POS/NEG_ACC_PEAK/MEAN/MEDIAN_GPS	Long. acc. peak, mean, median from GPS [g]
POS/NEG_ACC_25/50/75_PERC	25, 50, and 75 percentiles of long. acc. in the epoch [g]
POS/NEG_ACC_25/50/75_PERCTIME	Long. acc. at 25, 50, and 75 of the epoch duration in time [g]
POS/NEG_JERK_MIN/MAX	Long. jerk min and max [m/s^3]
POS/NEG_JERK_MEAN/MED_START_TO_PEAK	Long. jerk mean/median between start to peak [m/s^3]
POS/NEG_JERK_MEAN/MED_PEAK_TO_END	Long. jerk mean/median between peak to end [m/s^3]
POS/NEG_JERK_25/50/75_PERC	25, 50, and 75 percentiles of long. jerk in epoch [m/s^3]
POS/NEG_JERK_25/50/75_PERCTIME	Long. jerk at 25, 50, and 75 of epoch duration in time [m/s^3]
GPS_IMU_ERROR_PEAK	Percentage error between IMU and GPS peak acc. [%]
GPS_IMU_ERROR_MEAN	Percentage error between IMU and GPS mean acc. [%]
Specific metrics for roll rate epochs [NRR = negative roll rate; PRR = positive roll rate]	
PRR/NRR_ROLL_R_PEAK/MEAN/MEDIAN	Roll rate peak, mean, median [deg./sec.]
PRR/NRR_ROLL_R _25/50/75_PERC	25, 50, and 75 percentiles of roll rate in epoch [deg./sec.]
PRR/NRR_ROLL_R _25/50/75_PERCTIME	Roll rate at 25, 50, and 75 of epoch time duration [deg./sec.]
PRR/NRR_ROLL_PEAK/MEAN/MEDIAN	Roll mean, median in epoch [deg.]
PRR/NRR_START/END	Roll at start and end of epoch [deg.]
PRR/NRR_ROLL_25/50/75_PERC	25, 50, and 75 percentiles of roll. in epoch [deg.]
PRR/NRR_ROLL_25/50/75_PERCTIME	Roll at 25, 50, and 75 of the epoch time duration [deg.]

It is important to note that while acceleration/deceleration epochs captured the entire maneuver, roll rate epochs only encompassed half of the leaning maneuver, since a single roll rate epoch captures only one phase of the leaning maneuver—either into or out of the lean. Therefore, the mean roll value of each epoch was used to determine whether a roll rate epoch corresponded to the leaning-down phase or the recovery phase. To distinguish these epochs, the word "start" or "end" was added at the end of the roll rate-based metrics.

DATA ANALYSIS

The algorithm produced data summarization tables that were subsequently used to inform the study's research questions. To ensure that participants' riding data was sufficient to characterize individual riding styles and behaviors, participants who rode less than 500 miles were excluded from the analysis. The exclusion of low-mileage participants additionally mitigated potential biases arising from the predominance of specific travel routes (e.g., urban versus highway), which could skew comparisons across riders. As a result of this selection criterion, the final dataset included 122 participants out of the initial 155.

Normal riding behaviors and riding style clusters

The algorithm identified multiple epochs of acceleration, deceleration, positive roll-rate, and negative roll-rate, each characterized using the metrics listed in Table 1. To minimize bias from noise, coasting, and drag-related effects, acceleration and deceleration epochs were further filtered by including only those that met the following criteria: (1) the braking signal was active for deceleration epochs or inactive for acceleration epochs; (2) the epoch duration was less than 10 seconds; (3) the initial speed exceeded 10 mph; and (4) the difference between the mean deceleration measured by the IMU and the GPS was less than 25%.

To detect potential variations in riding styles among participants, this first analysis focused on two primary aspects of each epoch: (1) the mean, indicative of typical riding behavior, and (2) the peak, representative of extreme riding behavior. The distributions of these metrics were created for each participant, from which the mean and standard deviation were subsequently estimated. This process generated 16 metrics per rider, capturing both the central tendency and variability of maneuver intensity for each participant.

To reduce data dimensionality while preserving essential information and capturing the primary axes of variation, principal component analysis was performed on this set of participant-specific metrics. The resulting main components were then employed in a *k*-means cluster analysis to group participants based on similarities in their riding styles. Subsequently, statistical comparisons (analyses of variance [ANOVA] and χ^2) were conducted to determine whether the identified clusters exhibited statistically significant differences and to explore their association with key participant characteristics.

The clustering results were validated using time-headway data derived from radar measurements. Temporal separations between the ego-motorcycle and leading vehicles were computed after filtering out non-lead targets based on the radar unit's onboard logic. Time-headway distributions were then generated by aggregating participants according to their assigned clusters.

Association between rider kinematics and crash risk

To evaluate the relationship between specific kinematic metrics and crash risk, a bootstrap resampling framework was implemented. This approach repeatedly samples baseline trips for each event of interest, enabling robust statistical comparisons while compensating for the pronounced imbalance between CNC events and non-CNC trips.

The analysis began by designating CNC trips as the case group, while treating all other trips as the baseline pool (Figure 5). To enhance analytical accuracy, low-speed ground-impact crashes were excluded from the CNC group, as these events typically occurred during stationary conditions and reflected balance-loss crashes rather than active riding behavior. For each of the remaining 86 CNC trips, candidate baseline trips were selected from the non-CNC pool. Trip segments were selected from cases where the trip-level mean speed and distance was within a ±20% range of CNC trip selections. Baseline trip selection based on mean speed similarities served as a partial control for road types and traffic conditions. After this matching, all the acceleration and roll rate epochs were extracted for both CNC and baseline trips. A temporal clipping step then discarded epochs of the baseline trips which occurred after the percentile of trip duration at which the CNC event took place, ensuring temporal comparability between conditions.

For example, if the CNC occurred at 40% of the total CNC trip time-length, then only the baseline epochs occurring before the 40% of the total baseline trip time-length were retained. No data surrounding the CNC itself was included in the analysis. For each trip (both CNC and baseline), the mean and standard deviation of each epoch were calculated, and among all the baselines, 10 trips were randomly selected, minimizing missing data. Finally, summary statistics from the CNC trips and their matched baselines were compared with two-sample t-tests to identify significant deviations indicative of atypical riding behavior.

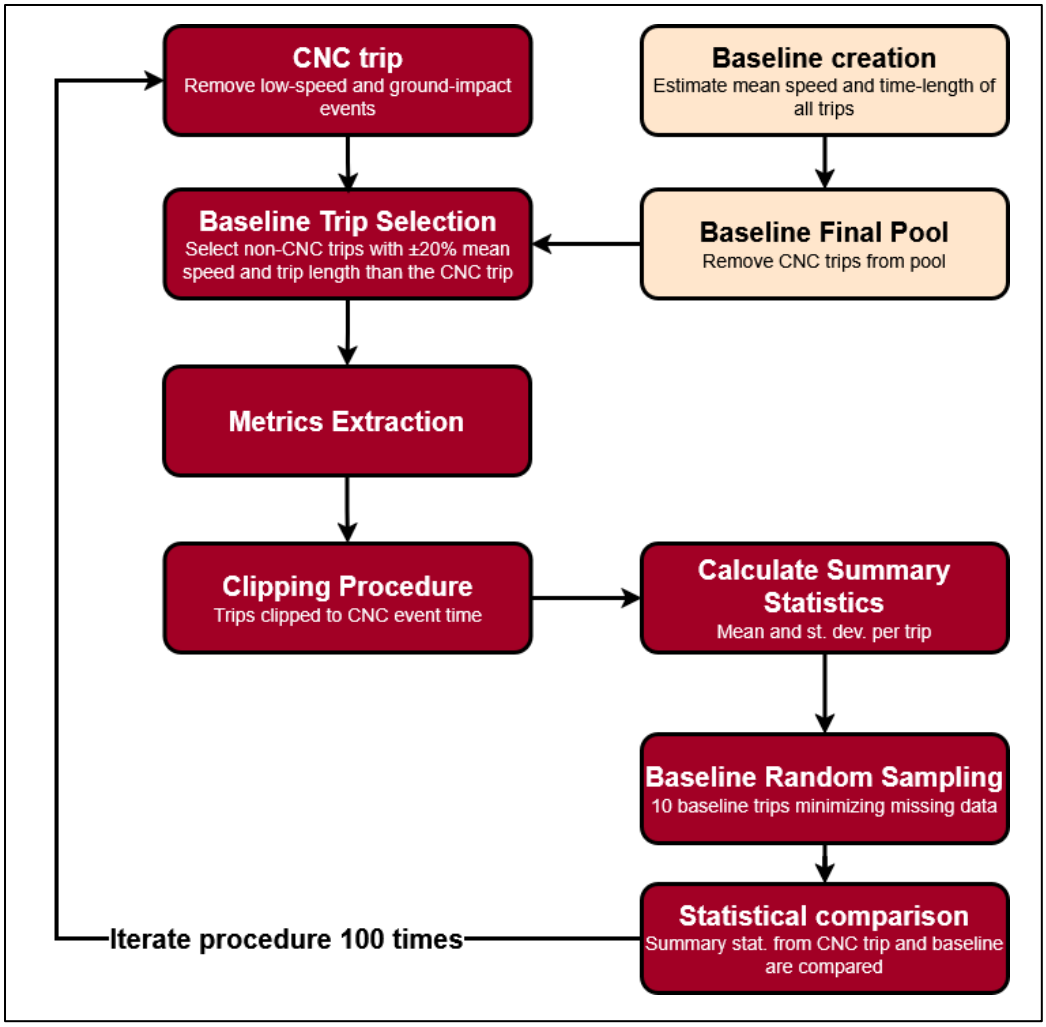

Figure 5. Flowchart. Bootstrap procedure.

The entire bootstrapping procedure was repeated 100 times, limiting the possibility that a particular single random draw of baseline trips would influence the statistical outcome.

CHAPTER 3. RESULTS

The kinematic analysis and clustering approach addressed the first research question by examining typical motorcycle riding behavior and characterizing it in terms of riding styles. The results in this section illustrate patterns of normal riding and individual variability among participants. The second research question is explored through the bootstrap analysis, which builds on these findings by linking abnormal riding behavior to increased crash risk.

MOTORCYCLE TYPICAL RIDING BEHAVIOR AND RIDING STYLE CLUSTERS

Typical riding behavior

The epoch-based algorithm identified thousands of unique kinematic epochs, allowing the exploration of possible correlations between the metrics collected. For example,

Figure 6 shows the increase of the epochs' mean deceleration values as a function of the speed reduction during the epoch.

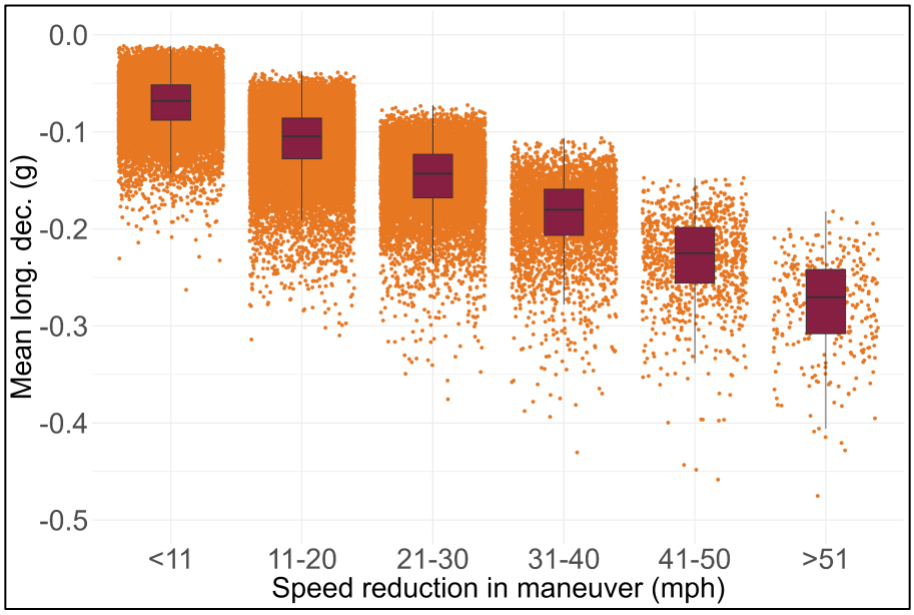

Figure 6. Graph. Mean longitudinal deceleration as a function of speed reduction in the maneuver.

The map matching analysis revealed that road classification and posted speed limits play a significant role in shaping the frequency of kinematic events, while exerting comparatively limited influence on the distributions (mean, quartiles) of their magnitude (see Figure A1-Appendix A).

The algorithm results also provide the foundation for understanding typical motorcycle riding behaviors. In terms of braking maneuvers, for example, the results revealed typical mean and peak deceleration values of approximately -0.1 g and -0.2 g (Figure 7), respectively, under normal riding conditions across the entire cohort of participants.

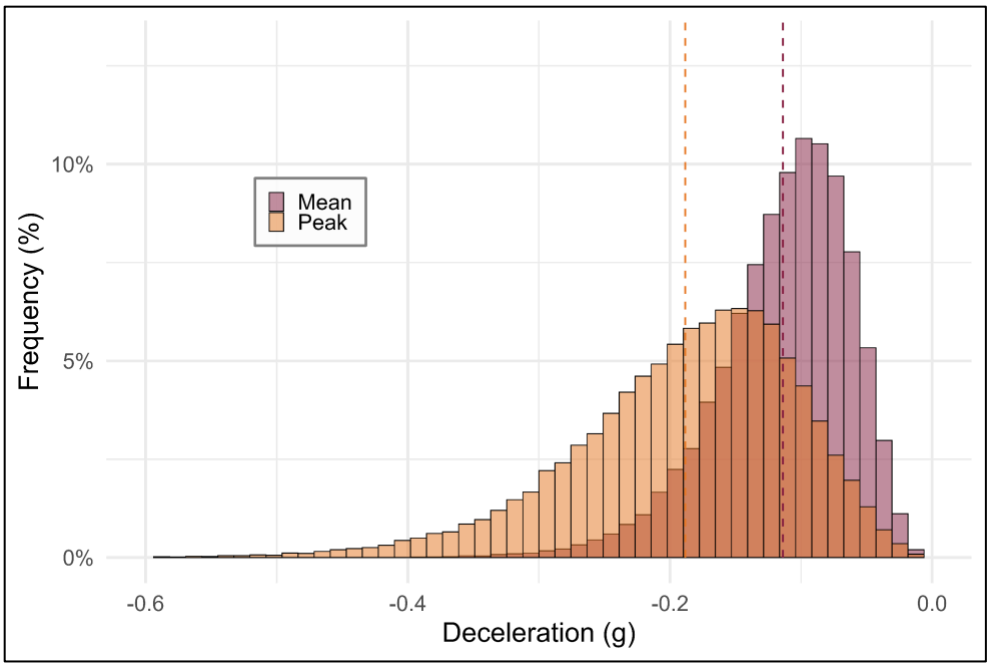

Figure 7. Graph. Distributions of mean and peak longitudinal decelerations during braking maneuvers across all participants and conditions.

The corresponding mean longitudinal jerk (first derivative of acceleration or how rapidly one is accelerating) is reported in Figure 8, differentiating between the mean value of the first part of the maneuver (before the peak of the acceleration) and the second part (after the peak).

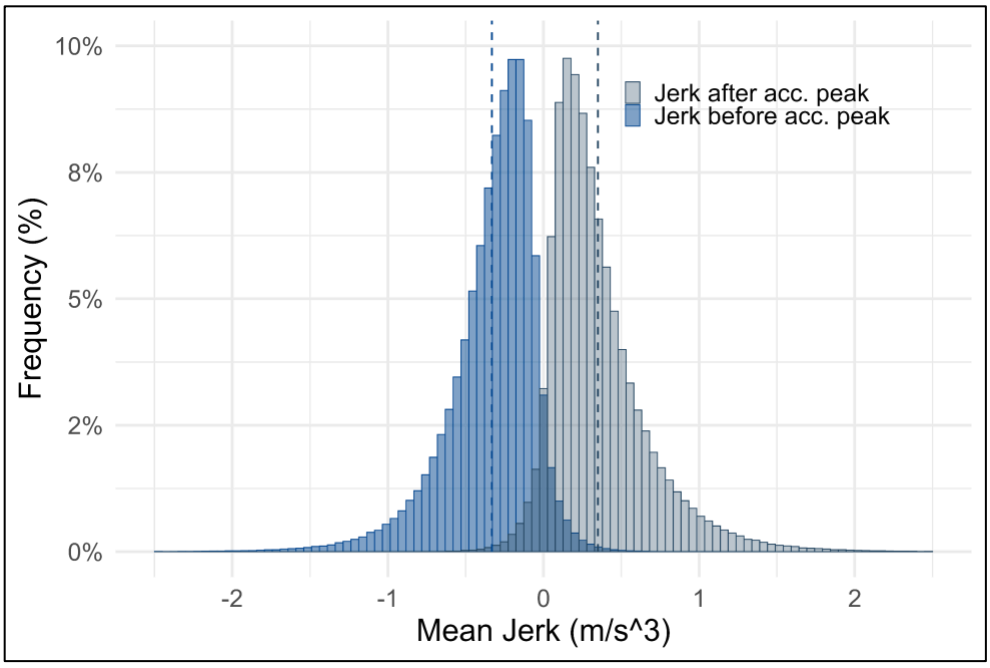

Figure 8. Graph. Distributions of the mean longitudinal jerks during braking maneuvers across all participants and conditions

While the kinematic distributions of the overall participants provided baseline behavior, significant individual variations emerged among the single participants. For example, Figure 9 shows the distributions of mean longitudinal deceleration during braking events for four participants. In this case, Participant D exhibited significantly higher mean deceleration values compared to the others, suggesting a more dynamic or sporty riding approach.

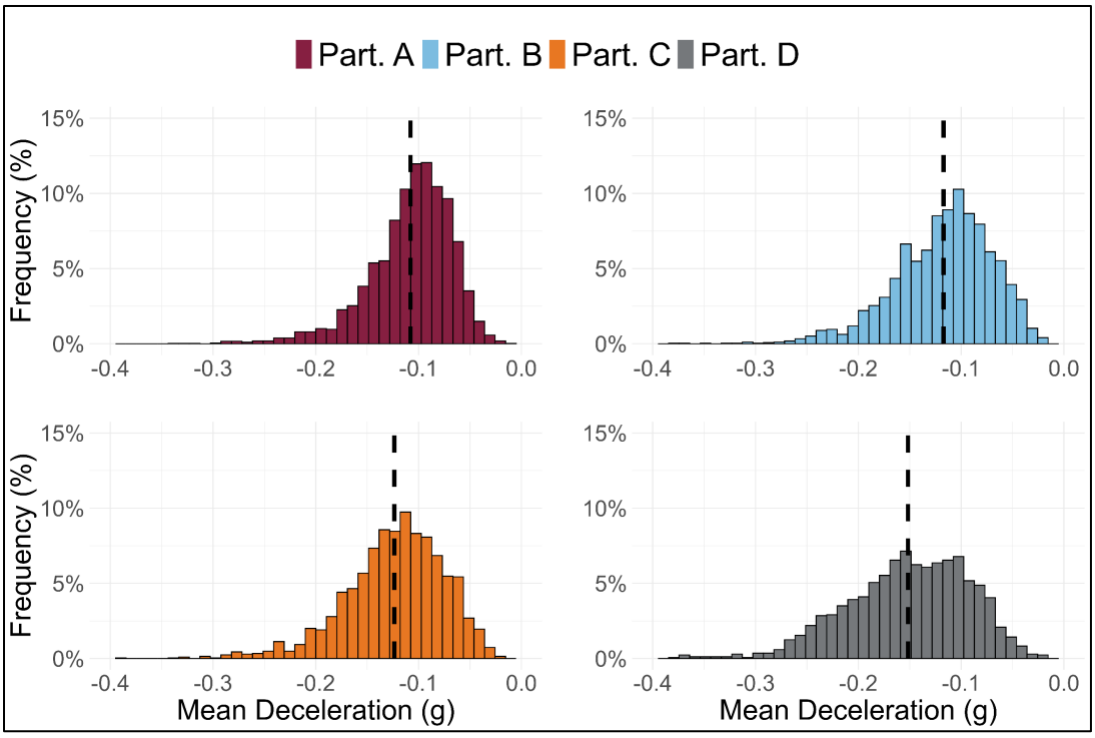

Figure 9. Graphs. Distributions of the mean longitudinal deceleration during braking events of four participants with corresponding mean values.

As with braking behavior, the distributions of positive longitudinal acceleration and roll rate revealed both similarities and differences among participants. These patterns, observed across the remaining 122 riders, motivated the development of a method to identify and distinguish subgroups based on their unique kinematic profiles.

Motorcycle riding styles

Figure 10 displays the box plots of the mean and peak longitudinal deceleration values for each rider. Notably, the inter-quartile ranges for deceleration were wider than those for positive accelerations, indicating that acceleration performance was relatively consistent across riders, whereas braking intensity had higher variability.

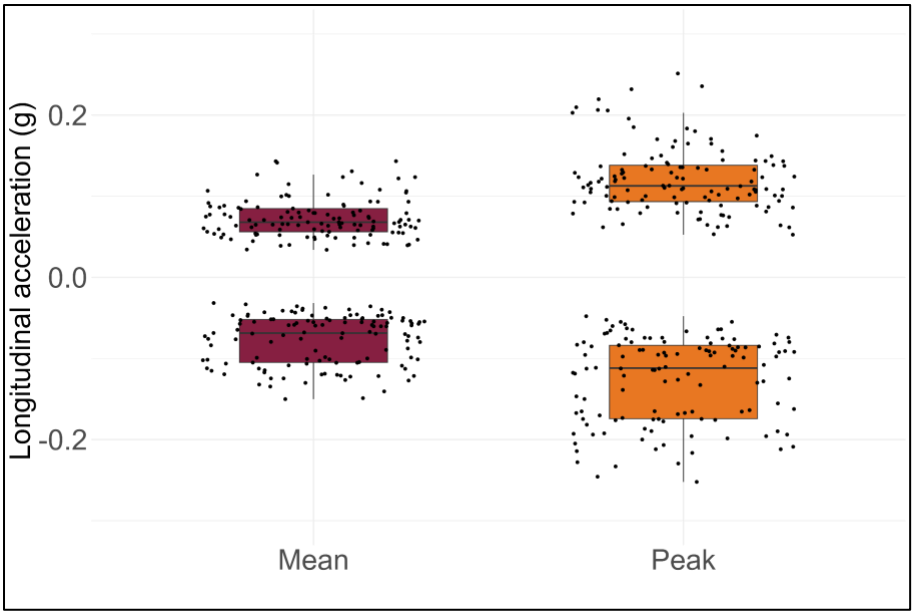

Figure 10. Box plots. Distribution of mean and peak longitudinal accelerations and decelerations for each participant.

The principal component analysis of the participants' aggregated mean and peak values showed that the first four components together captured more than 95% of the total variance (see Figure A2 – Appendix A). These four components were therefore used as inputs for the K-means clustering. The elbow criterion (see Figure A3 – Appendix A) indicated that a three-cluster solution (Figure 11) represented the best compromise between within-group consistency and overall model interpretability.

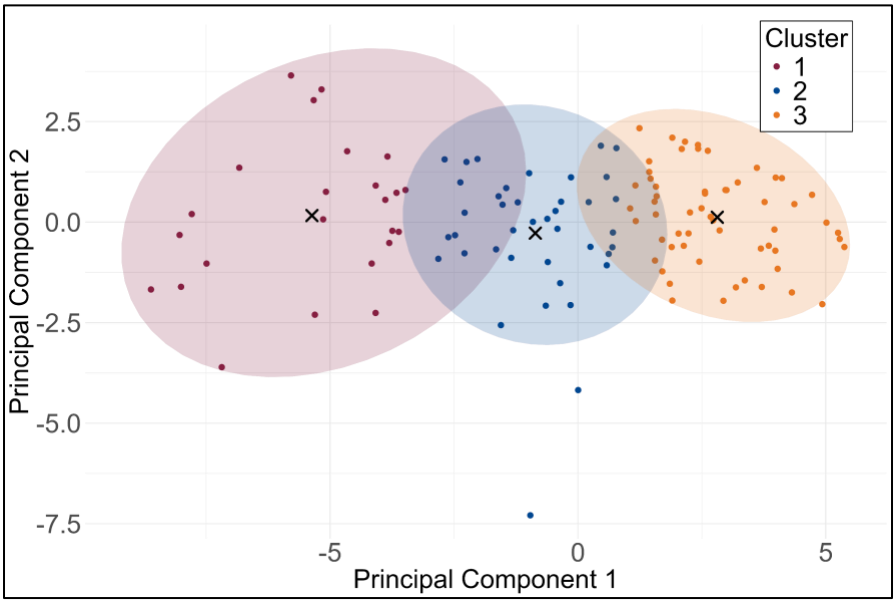

Figure 11. Scatterplot. The first two PCs with clusters assignments.

Figure 11 includes two observations from Cluster 2 that notably appear below the main PC2 distribution, indicating a potentially atypical kinematic behavior. The PC2 component exhibits strong positive loadings on the standard deviations of mean and peak acceleration/deceleration, alongside strong negative loadings on the mean roll-rate metrics. This suggests relatively consistent longitudinal kinematic behavior coupled with elevated mean roll rates for the two participants. To investigate potential bias, the raw data for these observations was carefully reviewed, and the distributions of the relevant metrics computed were compared to the overall sample. The review confirmed the low-variability/high-roll-rate profile but otherwise revealed no evidence of sensor drift or procedural error. Since these findings imply that the observed differences could represent genuine behavioral variations rather than artifacts, the observations were retained in all subsequent analyses. Nevertheless, all the analyses were repeated without these two participants to ensure robustness of the results: cluster compositions and statistical results were not affected, with only minimal changes in the numerical values of the cluster center of Cluster 2.

Assigning participants to these three clusters based on their PC scores produced distinct centroid profiles, each highlighting a unique pattern of longitudinal acceleration, deceleration, and roll-rate. Almost half of the sample (58 of 122 riders) belonged to Cluster 3, which was characterized by the gentle longitudinal inputs and the lowest positive and negative roll rates, indicating a cautious and smooth riding style. Conversely, riders in Clusters 1 and 2, although fewer in number, demonstrated stronger and more abrupt values for all the metrics (Table 2). The ANOVA indicated significant differences among clusters for all metrics. Specifically, Tukey's honestly significant difference post-hoc tests revealed that each cluster pair differed significantly across all metrics ($\alpha = 0.05$), confirming distinct and unique riding profiles and strategies among participants.

Table 2. Metrics results for the cluster centers.

Cluster Centers (122 riders)	Cluster 1 "Sporty" (24 riders)	Cluster 2 "Moderate" (40 riders)	Cluster 3 "Conservative" (58 riders)
Mean long. deceleration (g)	-0.12 ± 0.05	-0.09 ± 0.04	-0.05 ± 0.03
Peak long. deceleration (g)	-0.20 ± 0.09	-0.14 ± 0.07	-0.08 ± 0.06
Mean long. acceleration (g)	0.11 ± 0.08	0.07 ± 0.05	0.06 ± 0.04
Peak long. acceleration (g)	0.18 ± 0.13	0.12 ± 0.09	0.09 ± 0.07
Mean positive roll rate (deg/sec)	2.65 ± 2.05	2.14 ± 1.18	1.67 ± 0.56
Peak positive roll rate (deg/sec)	3.68 ± 3.22	2.89 ± 1.91	2.12 ± 0.91
Mean negative roll rate (deg/sec)	-2.41 ± 1.52	-2.09 ± 1.11	-1.69 ± 0.64
Peak negative roll rate (deg/sec)	-3.32 ± 2.45	-2.81 ± 1.83	-2.16 ± 1.08

The validation analysis examining radar data confirmed the cluster results, showing that conservative riders in Cluster 3 consistently maintained a greater distance from the vehicle ahead during car-following maneuvers, verifying that cluster's more cautious behavior compared to riders in the other clusters (Figure 12).

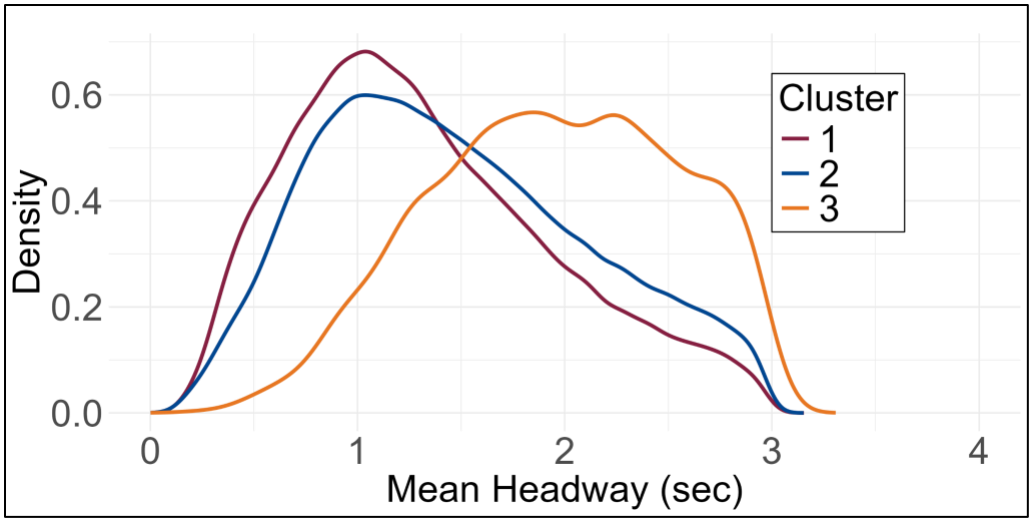

Figure 12. Graph. Distribution of the participants mean headway across clusters.

Table 3 provides the demographics and features of riders in each cluster, as well as the motorcycle characteristics and the extrapolated CNC rates per million vehicle miles traveled (MVMT). Cluster 1 was mainly composed of younger riders (mean age of 37 ± 12 years). Additionally, Cluster 1 also exhibited a substantially higher prevalence of sport motorcycles (92%). Conversely, Cluster 3 was composed of substantially older riders, with a mean age of 54 ± 13 years, and displayed the lowest proportion of sport motorcycles (16%).

Table 3. Summary statistics of participants' features per clusters.

Cluster	Age	Males (%)	Sport motorcycle (%)	Experienced riders (%)	High level training (%)	CNC rate per MVMT
1	37 (±12)	92	92	79	4	617 (±769)
2	41 (±12)	85	68	88	5	203 (±341)
3	54 (±13)	91	16	90	2	285 (±629)

Statistical analyses further underscored the importance of specific rider features. Participant age and motorcycle type differed significantly between Clusters 1 and 3 and between Clusters 2 and 3. However, despite the similarities between Clusters 1 and 2 in terms of rider age and percentage of sport motorcycle (see also Table 3), Cluster 1 had a notably higher average CNC rate (617 ± 769), roughly 2–3 times greater than the rates observed in Cluster 2 (203 ± 341) and Cluster 3 (285 ± 629). This suggests that differences in rider age and motorcycle type alone do not fully explain variations in riding performance or safety outcomes across clusters, suggesting inherent differences in riding style or behaviors among riders in the clusters. Other examined factors, such as male sex, rider experience, and high-level rider training, did not show statistically significant differences across clusters (Table 4).

Table 4. Summary of statistical test results assessing significant differences among clusters.

		Statistically different clusters (α = 0.05)		
Test variable	**Test statistics**	**1 vs 2**	**1 vs 3**	**2 vs 3**
CNC rate per MVMT	ANOVA + TukeyHSD	Yes	Yes	
Participant age	ANOVA + TukeyHSD		Yes	Yes
Motorcycle type presence	and pairwise proportions		Yes	Yes
Male sex presence	and pairwise proportions			
High experience presence	and pairwise proportions			
High training level presence	and pairwise proportions			

ASSOCIATION BETWEEN RIDER KINEMATICS AND CRASH RISK

The bootstrap analysis combined with a two-sample t-test investigated the deviations in the kinematic metrics preceding CNC events, highlighting longitudinal jerk during the initial phase of braking maneuvers as a key indicator of risky trips—evidenced by significant differences at specific points (e.g., the 25th percentile and 25% of epoch time), as well as in mean and median values over the maneuver's first half. A similar pattern was observed in positive acceleration maneuvers, where significant jerk value differences were also detected in the early part of the maneuver. In contrast, for roll rate, only the positive roll rate at 25% of the total length of the leaning-recovery phase was significantly different in 55 out of the 100 iterations, suggesting that motorcycle lateral kinematics may be less effective in identifying risky trips (Table 5). Notably, peak negative jerk resulted in significant differences in CNC cases vs baseline cases in 29% of the iterations, while peak values of acceleration and deceleration were never significantly different (Table A1 – Appendix A).

Table 5. Summary of bootstrap analysis results: metrics resulting in significant differences between CNC and non-CNC trips in more than 50 iterations.

Metrics used to compare CNC and baseline trips [POS = acceleration; NEG = deceleration; NRR = negative roll rate; PRR = positive roll rate]	**# of iterations resulting in statistical difference (N = 100)**
mean_NEG_JERK_25_PERCTIME_IMU	100
mean_NEG_JERK_25_PERC_IMU	100
std_NEG_JERK_25_PERC_IMU	100
std_NEG_JERK_MEDIAN_START_TO_PEAK_ACCEL_IMU	99
mean_NEG_JERK_MEDIAN_START_TO_PEAK_ACCEL_IMU	97
mean_NEG_JERK_MEAN_START_TO_PEAK_ACCEL_IMU	95
std_NEG_JERK_MEAN_START_TO_PEAK_ACCEL_IMU	94
std_NEG_JERK_25_PERCTIME_IMU	90
std_NEG_JERK_75_PERC_IMU	79
mean_POS_JERK_MEDIAN_START_TO_PEAK_ACCEL_IMU	71
mean_POS_JERK_MEAN_START_TO_PEAK_ACCEL_IMU	66
mean_PRR_ROLL_R_25_PERC_TIME_end	55

All these metrics exhibited a more extreme (higher mean and peak) behavior in CNC trips in comparison to baseline trips (see Figure 13).

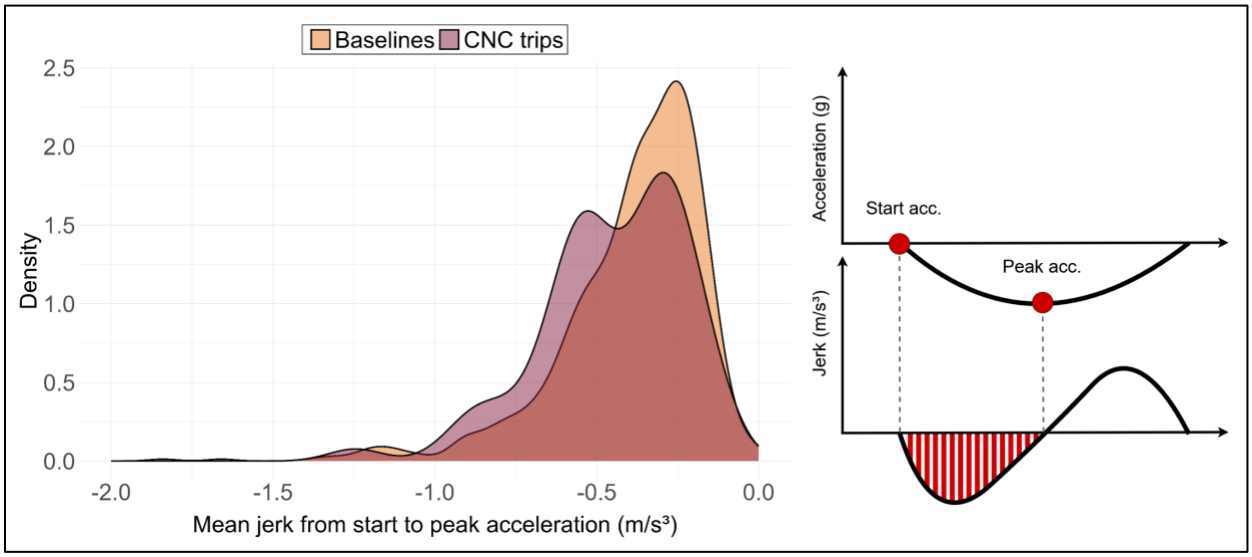

Figure 13. Graphs. Example of mean jerk during the initial phase of braking maneuvers.

CHAPTER 4. DISCUSSION

This study was successful in exploring both normal and abnormal riding, and associating those results to crashes, by using multiple commonly-available sensors. It provides novel insights into real-world motorcyclist behavior by identifying three distinct riding profiles characterized by unique kinematic patterns. Furthermore, several potential kinematic indicators that may predict crash risk were identified. This enhanced characterization of motorcycle rider capabilities could enable crash-scenario simulations with increased realism, inform evidence-based safety policies, help develop dynamic risk-scoring models for insurance companies, and support the design of advanced rider-assistance systems (ARAS) tailored to real-world parameters.

NORMAL RIDING BEHAVIOR AND RIDING STYLE CLUSTERS

The clustering of NRS data revealed substantial variability in rider performance, identifying three different groups of riders, which can be termed "Sporty," "Moderate," and "Conservative." Unlike previous studies, which predominantly focused on emergency riding responses (Davoodi & Hamid, 2013; Huertas-Leyva et al., 2019; Vavryn & Winkelbauer, 2004), the present work is the first to systematically characterize typical riding kinematics across a diverse rider population. While additional research is necessary to develop advanced modeling approaches for rider behavior, the cluster centroids and their distributions can be directly employed, for example, in simulation frameworks for emerging active-safety technologies (Lucci et al., 2021; Savino et al., 2013; Terranova et al., 2022).

Specifically, while mitigation-based technologies—such as automated emergency braking systems (Lucci et al., 2022)—would benefit from accurately modeling rider behaviors in emergency scenarios, support systems designed for regular riding tasks—like adaptive cruise control systems (Ait-moula et al., 2025)—can directly use the results of this study to closely emulate typical motorcycle riding capabilities. Furthermore, the parameterization of key motorcycle kinematics offers essential guidance for developers of passenger vehicle safety features and automated driving systems (ADSs). Extensive behavioral driving models exist for cars, heavy trucks, pedestrians, and micromobility vehicles (Dozza et al., 2023; Engström et al., 2024; Markkula, 2014; Terranova et al., 2024; Noonan et al., 2023), yet this study represents the first effort to model everyday motorcycle maneuvers using simplified methods. This work may facilitate the development of enhanced motorcycle rider models, enabling refinement of algorithms tailored specifically to motorcycles' unique operational characteristics. By integrating our kinematic profiles with established braking limits, researchers could create interaction scenarios involving motorcycles with increased realism, thereby enhancing the accuracy of crash probability assessments and ADS safety performance testing (Bareiss et al., 2019; Kusano et al., 2022).

Demographic and motorcycle-specific characteristics were closely associated with distinct riding styles identified within the clusters. Younger riders predominantly constituted the group characterized by the highest longitudinal acceleration and roll rate epochs but were dispersed across all three clusters. This is aligned with previous literature and could suggest a possible link between limited experience and lower risk perception (Keall & Newstead, 2012). In alignment with this, older riders were found to be overrepresented in the cluster with the lowest kinematic

metrics values, suggesting more conservative riding behaviors (Stephens et al., 2017). However, like the younger riders, older riders were present in all three clusters.

Similar to rider age, the predominant motorcycle type differed across clusters. Specifically, sport-motorcycle owners recorded significantly higher and more abrupt values across every kinematic metric, whereas cruiser and touring riders displayed smoother, more stable profiles. However, this finding warrants cautious interpretation, as sport motorcycles' performance-oriented design inherently amplifies metric values, potentially independently of actual rider behavior (Dunn et al., 2012). Further research is necessary to determine whether safety measures should be tailored specifically to motorcycle types. Despite their superior kinematic capabilities, sport motorcycle riders experienced a higher rate of CNC events per MVMT, suggesting that enhanced vehicle performance not only fails to mitigate their elevated crash exposure, but may also contribute to it. However, the convergence of sport bike ownership with young drivers within the highest-risk cluster underscores the urgent need for targeted interventions. Policies delaying unrestricted access to high-performance motorcycles, along with specialized training programs for young riders, could significantly reduce the disproportionate fatality rate among young sport motorcycle riders (Teoh & Campbell, 2010).

Rider sex, riding experience, and formal safety training did not significantly differentiate the clusters, a finding that contrasts with prior research emphasizing the protective role of experience against risky situations (Stephens et al., 2017) and its role in improving riding skills (Rainey et al., 2021; Rainey & McLaughlin, 2017). This discrepancy may stem from limited sample sizes within these demographic groups and potential biases inherent in self-reported rider experience (V. Williams et al., 2017).

The effects of map-related factors on kinematic events were examined and showed limited variation in magnitude across different road types and speed limits. In particular, a lower frequency of events was observed on higher-speed road categories (Figure A1 – Appendix A). These results are consistent with findings from car-based NDSs, which have repeatedly shown fewer acceleration events per mile on higher-speed roads (Ali et al., 2021, 2023). However, it is also possible that between-participant differences in map-related exposure—such as a tendency to ride more frequently on highways versus local roads—may have influenced the observed clusters. Therefore, future analyses should account for such between-participant variability to more accurately isolate the influence of road context on riding behavior.

ABNORMAL RIDING AND RISK BOOTSTRAP ANALYSIS

Previous naturalistic investigations on motorcycle data faced significant challenges in linking abnormal riding patterns to crash risk due to the absence of CNC events in collected datasets. Overcoming this limitation, the current study used a bootstrap analysis to compare kinematic metrics during CNC trips—in the period *preceding* the CNC event—with matched baseline trips without risky events. This approach provided a simple and robust method to identify riding behaviors predictive of elevated crash risk. The analysis identified the longitudinal jerk—defined as the rate of change in longitudinal acceleration—as the metric most strongly correlated with risky trips. This suggests that riders on high-risk trips exhibit more abrupt throttle and brake applications, resulting in rapid fluctuations in longitudinal acceleration. This result aligns with prior research on passenger cars, which identified sharp decelerations and high-jerk events as

critical indicators of safety-critical situations (Alrassy et al., 2023; M. Guo et al., 2022). While the current study did not directly investigate the possible causes of higher jerk values in CNC trips, research on passenger cars suggests that non-professional drivers exhibit more frequent high-jerk events, potentially due to limited experience and less refined vehicle control (Charly & Mathew, 2024). For motorcycles, similar factors—e.g., rider inexperience, distraction, or complex traffic conditions—may contribute to jerky riding patterns, although these hypotheses require further exploration.

Despite the need for future research, these findings have substantial practical implications for motorcycle safety. The identification of longitudinal jerk as a reliable surrogate measure of risk creates new opportunities for real-time safety evaluation frameworks (F. Guo et al., 2010). For instance, this metric could be integrated into telematics-based systems used by insurance companies to develop dynamic risk-scoring models. Such models would enable premiums to reflect real-time riding behavior rather than relying solely on static demographic factors, fostering more advanced pricing structures (Mao et al., 2021). Additionally, the findings have direct applications for the development of ARAS. Motorcycle manufacturers and ARAS developers could leverage jerk thresholds to design onboard alert systems that warn riders when their control inputs become abnormally abrupt, potentially preventing the escalation of risky behaviors and possibly mitigating crashes (Lisboa et al., 2024; Sevarin et al., 2020; Song et al., 2017; Terranova et al., 2022; Touliou et al., 2012).

Additionally, this study not only extends the relevance of longitudinal jerk as a key safety metric to the motorcycle domain but also highlights its predictive power for risk assessment when focusing on the initial phase of an epoch segment. This temporal specificity emphasizes the importance of early control inputs as critical precursors to hazardous riding behavior, providing a valuable opportunity for preventive interventions. This could suggest important opportunities for enhanced rider training programs. Training courses, for example, could focus on teaching smoothing initial control inputs during braking maneuvers, helping riders develop habits that mitigate the onset of high-risk behaviors. This could be particularly beneficial for novice riders, who may be more prone to abrupt throttle and brake applications due to inexperience (Aupetit et al., 2016; Huertas-Leyva et al., 2019, 2021).

CONCLUSIONS

This study presented a data-driven analysis of one of the largest NRS datasets collected to date, identifying three distinct riding styles and quantifying their different crash risks.

While the findings are promising, several limitations should be noted. Although longitudinal jerk emerged as a key predictor of crash risk, other kinematic variables—such as lateral acceleration and speeding behaviors—may also play a significant role and warrant further investigation. Furthermore, while riding styles were clustered based on mean and peak deceleration, future analyses should consider alternative surrogate metrics, such as the rate of high deceleration and events per mile, to better account for variations in trip characteristics (e.g., road types, speed limits, and traffic conditions).

Additionally, the relationship between rider demographics, environmental factors, and the occurrence of jerk-related events remains insufficiently explored. Future research should aim to model these complex interactions to uncover additional predictors of risky riding behavior.

Although the sample is geographically limited and under-represents female and specific motorcycle types, this approach demonstrates the feasibility of transforming raw kinematic data into actionable safety metrics. The resulting parameters provide developers, policymakers, and insurance companies with a realistic foundation for simulation, intervention design, and risk assessment, ultimately contributing to improved safety on U.S. roads.

APPENDIX A. ADDITIONAL GRAPHS

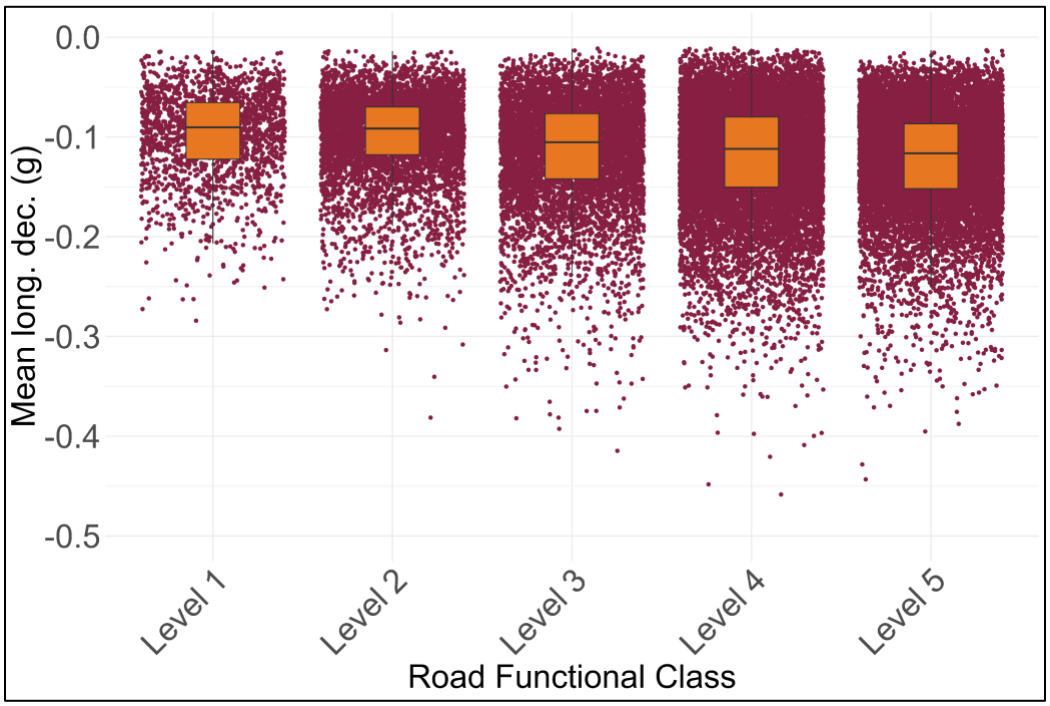

Figure A1. Mean longitudinal deceleration during braking events by road classification

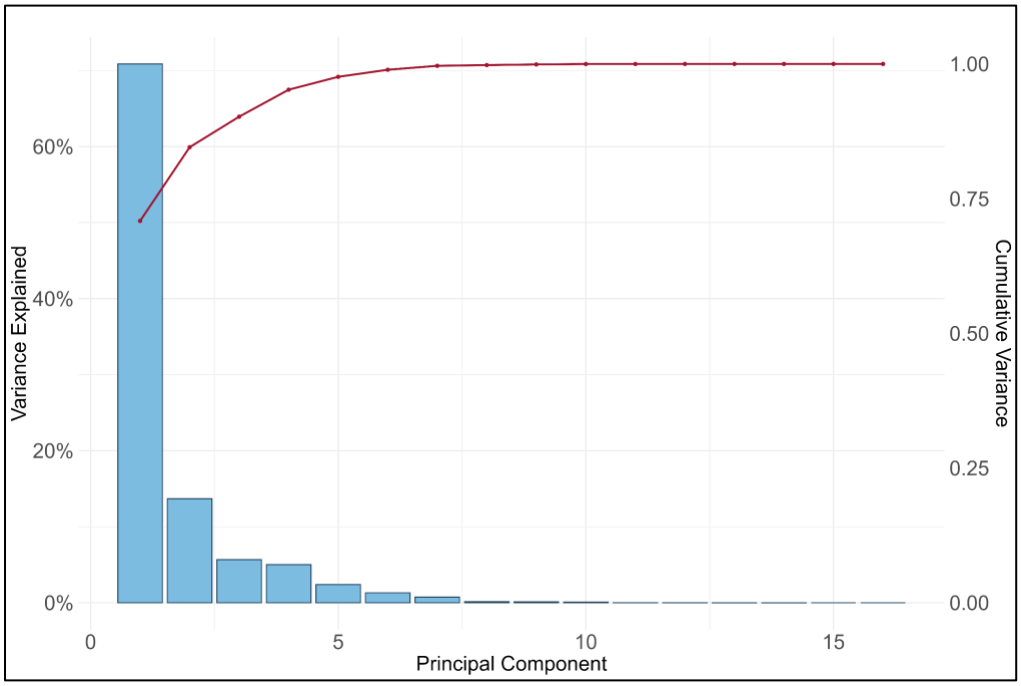

Figure A2. Variance explained and cumulative sum exaplained by the principal components.

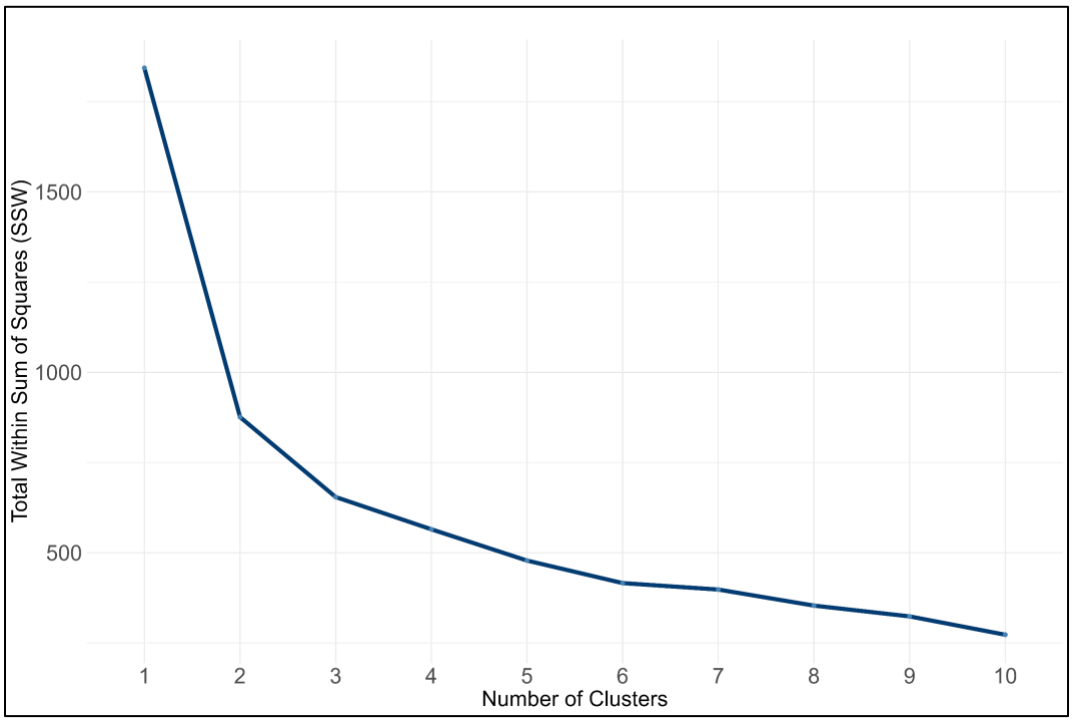

Figure A3. Elbow method representing the total within sum of squares (SSW) with respect to the number of clusers.

Table A1. Bootstrap analysis results: full list of metrics and number of iterations resulting in significant differences between CNC and non-CNC trips in at least 1 iteration out of 100.

Metric Name	# of iterations (out of 100)
mean_NEG_JERK_25_PERCTIME_IMU	100
mean_NEG_JERK_25_PERC_IMU	100
std_NEG_JERK_25_PERC_IMU	100
std_NEG_JERK_MEDIAN_START_TO_PEAK_ACCEL_IMU	99
mean_NEG_JERK_MEDIAN_START_TO_PEAK_ACCEL_IMU	97
mean_NEG_JERK_MEAN_START_TO_PEAK_ACCEL_IMU	95
std_NEG_JERK_MEAN_START_TO_PEAK_ACCEL_IMU	94
std_NEG_JERK_25_PERCTIME_IMU	90
std_NEG_JERK_75_PERC_IMU	79
mean_POS_JERK_MEDIAN_START_TO_PEAK_ACCEL_IMU	71
mean_POS_JERK_MEAN_START_TO_PEAK_ACCEL_IMU	66
mean_PRR_ROLL_R_25_PERC_TIME_end	55
std_POS_JERK_25_PERC_IMU	48
std_POS_ACC_25_PERCTIME_IMU	40
std_NEG_JERK_75_PERCTIME_IMU	40

Metric Name	# of iterations (out of 100)
std_POS_ACC_25_PERC_IMU	39
mean_POS_JERK_75_PERC_IMU	36
mean_NEG_JERK_MIN_IMU	29
mean_PRR_ROLL_R_75_PERC_end	26
mean_PRR_ROLL_R_PEAK_end	25
mean_PRR_ROLL_R_50_PERC_TIME_end	23
mean_PRR_ROLL_R_MEAN_end	21
std_NEG_JERK_MIN_IMU	19
std_POS_JERK_MEDIAN_PEAK_ACCEL_TO_END_IMU	17
mean_NEG_JERK_MEDIAN_PEAK_ACCEL_TO_END_IMU	16
mean_PRR_ROLL_R_50_PERC_end	15
mean_PRR_ROLL_R_MEDIAN_end	15
std_POS_ACC_MEAN_IMU	13
std_NEG_JERK_MAX_IMU	13
mean_PRR_ROLL_R_25_PERC_end	13
std_NRR_TIME_PEAK_ROLL_RATE_end	12
mean_POS_JERK_MAX_IMU	9
std_POS_JERK_MIN_IMU	9
std_POS_ACC_50_PERCTIME_IMU	8
std_POS_JERK_MEAN_PEAK_ACCEL_TO_END_IMU	8
mean_NEG_TIME_PEAK_ACC_IMU	7
std_POS_ACC_50_PERC_IMU	6
std_POS_ACC_MEDIAN_IMU	6
mean_NEG_JERK_50_PERC_IMU	6
mean_NEG_JERK_MEAN_PEAK_ACCEL_TO_END_IMU	5
mean_PRR_ROLL_INIT_init	4
std_POS_ACC_75_PERC_IMU	3
mean_POS_JERK_25_PERC_IMU	3
std_POS_TIME_PEAK_ACC_IMU	3
mean_NEG_JERK_50_PERCTIME_IMU	3
mean_NEG_ACC_50_PERCTIME_IMU	2
mean_NEG_ACC_50_PERC_IMU	2
mean_NEG_ACC_MEDIAN_IMU	2
std_NEG_JERK_MEAN_PEAK_ACCEL_TO_END_IMU	2
std_PRR_ROLL_R_50_PERC_TIME_init	2
mean_POS_JERK_50_PERCTIME_IMU	1
std_POS_JERK_75_PERCTIME_IMU	1
std_POS_JERK_MEAN_START_TO_PEAK_ACCEL_IMU	1
std_POS_JERK_MEDIAN_START_TO_PEAK_ACCEL_IMU	1
mean_NEG_ACC_25_PERC_IMU	1
mean_NEG_ACC_75_PERCTIME_IMU	1
mean_NEG_ACC_MEAN_GPS	1

Metric Name	# of iterations (out of 100)
mean_NEG_ACC_MEAN_IMU	1
std_NEG_ACC_PEAK_IMU	1
mean_NEG_ACC_SPEED_MEAN	1
mean_NEG_JERK_MAX_IMU	1
mean_NRR_ROLL_END_init	1
mean_PRR_ROLL_END_init	1

The following metrics were also evaluated but did not demonstrate predictive significance in any iteration.

mean_NEG_ACC_25_PERCTIME_IMU	mean_PRR_ROLL_25_PERC_TIME_init	std_NRR_ROLL_R_50_PERC_end
mean_NEG_ACC_75_PERC_IMU	mean_PRR_ROLL_50_PERC_end	std_NRR_ROLL_R_50_PERC_init
mean_NEG_ACC_PEAK_GPS	mean_PRR_ROLL_50_PERC_init	std_NRR_ROLL_R_50_PERC_TIME_end
mean_NEG_ACC_PEAK_IMU	mean_PRR_ROLL_50_PERC_TIME_end	std_NRR_ROLL_R_50_PERC_TIME_init
mean_NEG_JERK_75_PERC_IMU	mean_PRR_ROLL_50_PERC_TIME_init	std_NRR_ROLL_R_75_PERC_end
mean_NEG_JERK_75_PERCTIME_IMU	mean_PRR_ROLL_75_PERC_end	std_NRR_ROLL_R_75_PERC_init
mean_NRR_ROLL_25_PERC_end	mean_PRR_ROLL_75_PERC_init	std_NRR_ROLL_R_75_PERC_TIME_end
mean_NRR_ROLL_25_PERC_init	mean_PRR_ROLL_75_PERC_TIME_end	std_NRR_ROLL_R_75_PERC_TIME_init
mean_NRR_ROLL_25_PERC_TIME_end	mean_PRR_ROLL_75_PERC_TIME_init	std_NRR_ROLL_R_MEAN_end
mean_NRR_ROLL_25_PERC_TIME_init	mean_PRR_ROLL_END_end	std_NRR_ROLL_R_MEAN_init
mean_NRR_ROLL_50_PERC_end	mean_PRR_ROLL_INIT_end	std_NRR_ROLL_R_MEDIAN_end
mean_NRR_ROLL_50_PERC_init	mean_PRR_ROLL_MEADIAN_end	std_NRR_ROLL_R_MEDIAN_init
mean_NRR_ROLL_50_PERC_TIME_end	mean_PRR_ROLL_MEADIAN_init	std_NRR_ROLL_R_PEAK_end
mean_NRR_ROLL_50_PERC_TIME_init	mean_PRR_ROLL_MEAN_end	std_NRR_ROLL_R_PEAK_init
mean_NRR_ROLL_75_PERC_end	mean_PRR_ROLL_MEAN_init	std_NRR_TIME_PEAK_ROLL_RATE_init
mean_NRR_ROLL_75_PERC_init	mean_PRR_ROLL_R_25_PERC_init	std_POS_ACC_75_PERCTIME_IMU
mean_NRR_ROLL_75_PERC_TIME_end	mean_PRR_ROLL_R_25_PERC_TIME_init	std_POS_ACC_MEAN_GPS
mean_NRR_ROLL_75_PERC_TIME_init	mean_PRR_ROLL_R_50_PERC_init	std_POS_ACC_PEAK_GPS
mean_NRR_ROLL_END_end	mean_PRR_ROLL_R_50_PERC_TIME_init	std_POS_ACC_PEAK_IMU
mean_NRR_ROLL_INIT_end	mean_PRR_ROLL_R_75_PERC_init	std_POS_ACC_SPEED_MEAN
mean_NRR_ROLL_INIT_init	mean_PRR_ROLL_R_75_PERC_TIME_end	std_POS_JERK_25_PERCTIME_IMU
mean_NRR_ROLL_MEADIAN_end	mean_PRR_ROLL_R_75_PERC_TIME_init	std_POS_JERK_50_PERC_IMU
mean_NRR_ROLL_MEADIAN_init	mean_PRR_ROLL_R_MEAN_init	std_POS_JERK_50_PERCTIME_IMU
mean_NRR_ROLL_MEAN_end	mean_PRR_ROLL_R_MEDIAN_init	std_POS_JERK_75_PERC_IMU
mean_NRR_ROLL_MEAN_init	mean_PRR_ROLL_R_PEAK_init	std_POS_JERK_MAX_IMU
mean_NRR_ROLL_R_25_PERC_end	mean_PRR_TIME_PEAK_ROLL_RATE_end	std_PRR_ROLL_25_PERC_end
mean_NRR_ROLL_R_25_PERC_init	mean_PRR_TIME_PEAK_ROLL_RATE_init	std_PRR_ROLL_25_PERC_init
mean_NRR_ROLL_R_25_PERC_TIME_end	std_NEG_ACC_25_PERC_IMU	std_PRR_ROLL_25_PERC_TIME_end
mean_NRR_ROLL_R_25_PERC_TIME_init	std_NEG_ACC_25_PERCTIME_IMU	std_PRR_ROLL_25_PERC_TIME_init
mean_NRR_ROLL_R_50_PERC_end	std_NEG_ACC_50_PERC_IMU	std_PRR_ROLL_50_PERC_end
mean_NRR_ROLL_R_50_PERC_init	std_NEG_ACC_50_PERCTIME_IMU	std_PRR_ROLL_50_PERC_init
mean_NRR_ROLL_R_50_PERC_TIME_end	std_NEG_ACC_75_PERC_IMU	std_PRR_ROLL_50_PERC_TIME_end
mean_NRR_ROLL_R_50_PERC_TIME_init	std_NEG_ACC_75_PERCTIME_IMU	std_PRR_ROLL_50_PERC_TIME_init
mean_NRR_ROLL_R_75_PERC_end	std_NEG_ACC_MEAN_GPS	std_PRR_ROLL_75_PERC_end
mean_NRR_ROLL_R_75_PERC_init	std_NEG_ACC_MEAN_IMU	std_PRR_ROLL_75_PERC_init
mean_NRR_ROLL_R_75_PERC_TIME_end	std_NEG_ACC_MEDIAN_IMU	std_PRR_ROLL_75_PERC_TIME_end
mean_NRR_ROLL_R_75_PERC_TIME_init	std_NEG_ACC_PEAK_GPS	std_PRR_ROLL_75_PERC_TIME_init
mean_NRR_ROLL_R_MEAN_end	std_NEG_ACC_SPEED_MEAN	std_PRR_ROLL_END_end
mean_NRR_ROLL_R_MEAN_init	std_NEG_JERK_50_PERC_IMU	std_PRR_ROLL_END_init
mean_NRR_ROLL_R_MEDIAN_end	std_NEG_JERK_50_PERCTIME_IMU	std_PRR_ROLL_INIT_end
mean_NRR_ROLL_R_MEDIAN_init	std_NEG_JERK_MEDIAN_PEAK_ACCEL_TO_END_IMU	std_PRR_ROLL_INIT_init
mean_NRR_ROLL_R_PEAK_end	std_NEG_TIME_PEAK_ACC_IMU	std_PRR_ROLL_MEADIAN_end
mean_NRR_ROLL_R_PEAK_init	std_NRR_ROLL_25_PERC_end	std_PRR_ROLL_MEADIAN_init
mean_NRR_TIME_PEAK_ROLL_RATE_end	std_NRR_ROLL_25_PERC_init	std_PRR_ROLL_MEAN_end
mean_NRR_TIME_PEAK_ROLL_RATE_init	std_NRR_ROLL_25_PERC_TIME_end	std_PRR_ROLL_MEAN_init
mean_POS_ACC_25_PERC_IMU	std_NRR_ROLL_25_PERC_TIME_init	std_PRR_ROLL_R_25_PERC_end
mean_POS_ACC_50_PERC_IMU	std_NRR_ROLL_50_PERC_end	std_PRR_ROLL_R_25_PERC_init
mean_POS_ACC_50_PERCTIME_IMU	std_NRR_ROLL_50_PERC_init	std_PRR_ROLL_R_25_PERC_TIME_end
mean_POS_ACC_75_PERC_IMU	std_NRR_ROLL_50_PERC_TIME_end	std_PRR_ROLL_R_25_PERC_TIME_init
mean_POS_ACC_75_PERCTIME_IMU	std_NRR_ROLL_50_PERC_TIME_init	std_PRR_ROLL_R_50_PERC_end
mean_POS_ACC_MEAN_GPS	std_NRR_ROLL_75_PERC_end	std_PRR_ROLL_R_50_PERC_init
mean_POS_ACC_MEAN_IMU	std_NRR_ROLL_75_PERC_init	std_PRR_ROLL_R_50_PERC_TIME_end
mean_POS_ACC_MEDIAN_IMU	std_NRR_ROLL_75_PERC_TIME_end	std_PRR_ROLL_R_75_PERC_end
mean_POS_ACC_PEAK_GPS	std_NRR_ROLL_75_PERC_TIME_init	std_PRR_ROLL_R_75_PERC_init
mean_POS_ACC_PEAK_IMU	std_NRR_ROLL_END_end	std_PRR_ROLL_R_75_PERC_TIME_end
mean_POS_ACC_SPEED_MEAN	std_NRR_ROLL_END_init	std_PRR_ROLL_R_75_PERC_TIME_init
mean_POS_JERK_25_PERCTIME_IMU	std_NRR_ROLL_INIT_end	std_PRR_ROLL_R_MEAN_end

mean_POS_JERK_50_PERC_IMU	std_NRR_ROLL_INIT_init	std_PRR_ROLL_R_MEAN_init
mean_POS_JERK_75_PERCTIME_IMU	std_NRR_ROLL_MEADIAN_end	std_PRR_ROLL_R_MEDIAN_end
mean_POS_JERK_MEAN_PEAK_ACCEL_TO_END_IMU	std_NRR_ROLL_MEADIAN_init	std_PRR_ROLL_R_MEDIAN_init
mean_POS_JERK_MEDIAN_PEAK_ACCEL_TO_END_IMU	std_NRR_ROLL_MEAN_end	std_PRR_ROLL_R_PEAK_end
mean_POS_JERK_MIN_IMU	std_NRR_ROLL_MEAN_init	std_PRR_ROLL_R_PEAK_init
mean_POS_TIME_PEAK_ACC_IMU	std_NRR_ROLL_R_25_PERC_end	std_PRR_TIME_PEAK_ROLL_RATE_end
mean_PRR_ROLL_25_PERC_end	std_NRR_ROLL_R_25_PERC_init	std_PRR_TIME_PEAK_ROLL_RATE_init
mean_PRR_ROLL_25_PERC_init	std_NRR_ROLL_R_25_PERC_TIME_end	
mean_PRR_ROLL_25_PERC_TIME_end	std_NRR_ROLL_R_25_PERC_TIME_init	

REFERENCES

Ait-moula, A., Naude, C., Riahi, E., & Serre, T. (2025). Enhancing motorcycle safety: Quantifying the effects of Autonomous Emergency Braking and Adaptive Cruise Control in crashes reduction. *Traffic Injury Prevention*, 1–10. https://doi.org/10.1080/15389588.2025.2461575

Ali, G. (2023). *Characterizing human driving behavior through an analysis of naturalistic driving data* [Dissertation, Virginia Tech].

Ali, G., McLaughlin, S., & Ahmadian, M. (2021). Quantifying the effect of roadway, driver, vehicle, and location characteristics on the frequency of longitudinal and lateral accelerations. *Accident Analysis & Prevention*, *161*, 106356. https://doi.org/10.1016/j.aap.2021.106356

Ali, G., McLaughlin, S., & Ahmadian, M. (2023). The Surface Accelerations Reference—A Large-Scale, Interactive Catalog of Passenger Vehicle Accelerations. *IEEE Transactions on Intelligent Transportation Systems*, *24*(9), 9031–9040. https://doi.org/10.1109/TITS.2023.3267844

Alrassy, P., Smyth, A. W., & Jang, J. (2023). Driver behavior indices from large-scale fleet telematics data as surrogate safety measures. *Accident Analysis & Prevention*, *179*, 106879. https://doi.org/10.1016/j.aap.2022.106879

Aupetit, S., Gallier, V., Riff, J., Espié, S., & Delgehier, F. (2016). Naturalistic study of the risky situations faced by novice riders. *Ergonomics*, *59*(8), 1109–1120. https://doi.org/10.1080/00140139.2015.1120887

Aupetit, S., Riff, J., Buttelli, O., & Espié, S. (2013). Naturalistic study of rider's behaviour in initial training in France: Evidence of limitations in the educational content. *Accident Analysis and Prevention*, *58*, 206–217. https://doi.org/10.1016/j.aap.2012.09.036

Baldanzini, N., Huertas-Leyva, P., Savino, G., & Pierini, M. (2016). Rider Behavioral Patterns in Braking Manoeuvres. *Transportation Research Procedia*, *14*, 4374–4383. https://doi.org/10.1016/j.trpro.2016.05.359

Bareiss, M., Scanlon, J., Sherony, R., & Gabler, H. C. (2019). Crash and injury prevention estimates for intersection driver assistance systems in left turn across path/opposite direction crashes in the United States. *Traffic Injury Prevention*, *20*(sup1), S133–S138. https://doi.org/10.1080/15389588.2019.1610945

Bartolozzi, M., Boubezoul, A., Bouaziz, S., Savino, G., & Espié, S. (2023). Understanding the behaviour of motorcycle riders: An objective investigation of riding style and capability. *Transportation Research Interdisciplinary Perspectives*, *22*. https://doi.org/10.1016/j.trip.2023.100971

Boer, E. R., Nobuyuki, K., & Tomohiro, Y. (2001). Affording realistic stopping behavior: A cardinal challenge for driving simulators. *Proceedings of 1st Human-Centered Transportation Simulation Conference*.

Charly, A., & Mathew, T. V. (2024). Identifying risky driving behavior: a field study using instrumented vehicles. *Transportation Letters*, *16*(7), 688–702. https://doi.org/10.1080/19427867.2023.2233782

Crundall, E., Stedmon, A. W., Saikayasit, R., & Crundall, D. (2013). A simulator study investigating how motorcyclists approach side-road hazards. *Accident Analysis & Prevention*, *51*, 42–50. https://doi.org/10.1016/j.aap.2012.10.017

Davoodi, S. R., & Hamid, H. (2013). Motorcyclist Braking Performance in Stopping Distance Situations. *Journal of Transportation Engineering*, *139*(7), 660–666. https://doi.org/10.1061/(ASCE)TE.1943-5436.0000552

Davoodi, S. R., Hamid, H., Pazhouhanfar, M., & Muttart, J. W. (2012). Motorcyclist perception response time in stopping sight distance situations. *Safety Science*, *50*(3), 371–377. https://doi.org/10.1016/j.ssci.2011.09.004

Deligianni, S. P., Quddus, M., Morris, A., Anvuur, A., & Reed, S. (2017). Analyzing and Modeling Drivers' Deceleration Behavior from Normal Driving. *Transportation Research Record: Journal of the Transportation Research Board*, *2663*(1), 134–141. https://doi.org/10.3141/2663-17

Dingus, T. A., Guo, F., Lee, S., Antin, J. F., Perez, M., Buchanan-King, M., & Hankey, J. (2016). Driver crash risk factors and prevalence evaluation using naturalistic driving data. *Proceedings of the National Academy of Sciences*, *113*(10), 2636–2641. https://doi.org/10.1073/pnas.1513271113

Diop, M., Boubezoul, A., Oukhellou, L., Espié, S., & Bouaziz, S. (2023). Powered Two-Wheelers Right-Hand Curve Negotiation Study Using Segmentation and Data Mining Approaches. *IEEE Transactions on Intelligent Transportation Systems*, *24*(3), 3407–3421. https://doi.org/10.1109/TITS.2022.3222421

Dozza, M., Li, T., Billstein, L., Svernlöv, C., & Rasch, A. (2023). How do different micro-mobility vehicles affect longitudinal control? Results from a field experiment. *Journal of Safety Research*, *84*, 24–32. https://doi.org/10.1016/j.jsr.2022.10.005

Dunn, A. L., Dorohoff, M., Bayan, F., Cornetto, A., Wahba, R., Chuma, M., Guenther, D. A., & Eiselstein, N. (2012, April 16). *Analysis of Motorcycle Braking Performance and Associated Braking Marks*. https://doi.org/10.4271/2012-01-0610

Engström, J., Liu, S.-Y., Dinparastdjadid, A., & Simoiu, C. (2024). Modeling road user response timing in naturalistic traffic conflicts: A surprise-based framework. *Accident Analysis & Prevention*, *198*, 107460. https://doi.org/10.1016/j.aap.2024.107460

Espié, S., Boubezoul, A., Aupetit, S., & Bouaziz, S. (2013). Data collection and processing tools for naturalistic study of powered two-wheelers users' behaviours. *Accident Analysis and Prevention*, *58*, 330–339. https://doi.org/10.1016/j.aap.2013.03.012

Guo, F., Klauer, S. G., Hankey, J. M., & Dingus, T. A. (2010). Near Crashes as Crash Surrogate for Naturalistic Driving Studies. *Transportation Research Record: Journal of the Transportation Research Board*, *2147*(1), 66–74. https://doi.org/10.3141/2147-09

Guo, M., Zhao, X., Yao, Y., Bi, C., & Su, Y. (2022). Application of risky driving behavior in crash detection and analysis. *Physica A: Statistical Mechanics and Its Applications*, *591*, 126808. https://doi.org/10.1016/j.physa.2021.126808

HERE Maps XML. (2025). *Functional Class*. Https://Www.Here.Com/Docs/Bundle/Maps-Xml-Data-Specification/Page/Format-Agnostic-Data/Format_agnostic_data_specification/Topics/Ra-Functional-Class.Html.

Huertas-Leyva, P., Baldanzini, N., Savino, G., & Pierini, M. (2021). Human error in motorcycle crashes: A methodology based on in-depth data to identify the skills needed and support training interventions for safe riding. *Traffic Injury Prevention*, *22*(4), 294–300. https://doi.org/10.1080/15389588.2021.1896714

Huertas-Leyva, P., Nugent, M., Savino, G., Pierini, M., Baldanzini, N., & Rosalie, S. (2019). Emergency braking performance of motorcycle riders: skill identification in a real-life perception-action task designed for training purposes. *Transportation Research Part F: Traffic Psychology and Behaviour*, *63*, 93–107. https://doi.org/10.1016/j.trf.2019.03.019

Ibrahim, M. K. A., Siam, M. F. M., Fin, L. S., & Ishak, S. Z. (2019). Large-Scale Naturalistic Riding Data Collection: A Pilot Study. Malaysian Institute of Road Safety Research (MIROS).

Jain, S., & Perez, M. A. (2025). On-Road Evaluation of an Unobtrusive In-Vehicle Pressure-Based Driver Respiration Monitoring System. *Sensors*, *25*(9), 2739. https://doi.org/10.3390/s25092739

Jamson, A. H., & Smith, P. (2003). Are You Used To It Yet? Braking Performance and Adaptation in a Fixed-base Driving Simulator. *Driving Simulation Conference North, America (DSC-NA 2003)*.

Keall, M. D., & Newstead, S. (2012). Analysis of factors that increase motorcycle rider risk compared to car driver risk. *Accident Analysis & Prevention*, *49*, 23–29. https://doi.org/10.1016/j.aap.2011.07.001

Kovácsová, N., Grottoli, M., Celiberti, F., Lemmens, Y., Happee, R., Hagenzieker, M. P., & de Winter, J. C. F. (2020). Emergency braking at intersections: A motion-base motorcycle simulator study. *Applied Ergonomics*, *82*, 102970. https://doi.org/10.1016/j.apergo.2019.102970

Kumar Akinapalli, P., Pawar, D. S., & Dia, H. (2023). Classification of motorized two-wheeler riders' acceleration and deceleration behavior through short-term naturalistic riding study. *Transportation Research Part F: Traffic Psychology and Behaviour*, *96*, 92–110. https://doi.org/10.1016/j.trf.2023.06.008

Kusano, K. D., Beatty, K., Schnelle, S., Favaro, F., Crary, C., & Victor, T. (2022). Collision avoidance testing of the waymo automated driving system. *ArXiv Preprint* ArXiv:2212.08148.

Limebeer, D. J. N., Sharp, R. S., & Evangelou, S. (2001). The stability of motorcycles under acceleration and braking. *Proceedings of the Institution of Mechanical Engineers, Part C: Journal of Mechanical Engineering Science*, *215*(9), 1095–1109. https://doi.org/10.1177/095440620121500910

Lisboa, I. C., Lourenço, V., Silva, E., Pereira, E., Carvalho, A., Pessoa, R., & Costa, N. (2024). Haptic warnings for a motorcycle jacket and gloves. *Transportation Research Part F: Traffic Psychology and Behaviour*, *100*, 197–210. https://doi.org/10.1016/j.trf.2023.11.017

Lucci, C., Allen, T., Pierini, M., & Savino, G. (2021). Motorcycle Autonomous Emergency Braking (MAEB) employed as enhanced braking: Estimating the potential for injury reduction using real-world crash modeling. *Traffic Injury Prevention*, *22*(sup1), S104–S110. https://doi.org/10.1080/15389588.2021.1960319

Lucci, C., Savino, G., & Baldanzini, N. (2022). Does Motorcycle Autonomous Emergency Braking (MAEB) mitigate rider injuries and fatalities? Design of effective working parameters and field test validation of their acceptability. *Transportation Research Part C: Emerging Technologies*, *145*, 103865. https://doi.org/10.1016/j.trc.2022.103865

Magiera, N., Janssen, H., Heckmann, M., & Winner, H. (2016). Rider skill identification by probabilistic segmentation into motorcycle maneuver primitives. *2016 IEEE 19th International Conference on Intelligent Transportation Systems (ITSC)*, 379–386. https://doi.org/10.1109/ITSC.2016.7795583

Mao, H., Guo, F., Deng, X., & Doerzaph, Z. R. (2021). Decision-adjusted driver risk predictive models using kinematics information. *Accident Analysis & Prevention*, *156*, 106088. https://doi.org/10.1016/j.aap.2021.106088

Markkula, G. (2014). Modeling driver control behavior in both routine and near-accident driving. *Proceedings of the Human Factors and Ergonomics Society Annual Meeting*, *58*(1), 879–883. https://doi.org/10.1177/1541931214581185

McCall, R., McLaughlin, S., Williams, S., & Buche, T. (2014). Analysis of temperature and precipitation data in naturalistic motorcycle study. *Proceedings of the Human Factors and Ergonomics Society*, *2014-January*, 2117–2121. https://doi.org/10.1177/1541931214581445

McCall, R., McLaughlin, S., Williams, V., Rainey, C., Fritz, S. (in press). *Instrumented On-Road Study of Motorcycle Riders Volume 3: The Relationship between Exposure, Geometry and Crash/Near-Crash Risk* (DOT # pending). National Highway Traffic Safety Administration.

National Highway Traffic Safety Administration. (2019). *Motorcycle Safety 5-Year Plan – 2019*.

National Highway Traffic Safety Administration. (2024a). *Motorcycles: 2022 data*.

National Highway Traffic Safety Administration. (2024b). *Traffic safety facts 2022: A compilation of motor vehicle traffic crash data*.

National Highway Traffic Safety Administration. (2024). *Overview of motor vehicle traffic crashes in 2022*.

Nugent, M., Savino, G., Mulvihill, C., Lenné, M., & Fitzharris, M. (2019). Evaluating rider steering responses to an unexpected collision hazard using a motorcycle riding simulator. *Transportation Research Part F: Traffic Psychology and Behaviour*, *66*, 292–309. https://doi.org/10.1016/j.trf.2019.09.005

Penumaka, A. P., Savino, G., Baldanzini, N., & Pierini, M. (2014). In-depth investigations of PTW-car accidents caused by human errors. *Safety Science*, *68*, 212–221. https://doi.org/10.1016/j.ssci.2014.04.004

Perez, M. A., Terranova, P., Metrey, M., Bragg, H., & Britten, N. (2024). *Characterizing Level 2 Automation in a Naturalistic Driving Fleet*. Virginia Tech Transportation Institute. https://hdl.handle.net/10919/118141

Puthan, P., Lubbe, N., Shaikh, J., Sui, B., & Davidsson, J. (2021). Defining crash configurations for Powered Two-Wheelers: Comparing ISO 13232 to recent in-depth crash data from Germany, India and China. *Accident Analysis & Prevention*, *151*, 105957. https://doi.org/10.1016/j.aap.2020.105957

Rainey, C., & McLaughlin, S. (2017). A Naturalistic Look at Motorcyclist Acceleration and Deceleration Behaviour. In *Presentation at The 6th International Naturalistic Driving Research Symposium*.

Rainey, C., McLaughlin, S., & Williams, L. (2014). Analysis of Mean Trip Speed of Motorcycle Riders. *Fourth International Symposium on Naturalistic Driving Research*.

Rainey, C., Williams, V., McLaughlin, S., & Buche, T. (2021). Deceleration Differences Between Novice and Experienced Riders. In *Presentation*.

Sakashita, C., Senserrick, T., Lo, S., Boufous, S., Rome, L. de, & Ivers, R. (2014). The Motorcycle Rider Behavior Questionnaire: Psychometric properties and application amongst novice riders in Australia. *Transportation Research Part F: Traffic Psychology and Behaviour*, *22*, 126–139. https://doi.org/10.1016/j.trf.2013.10.005

Sarkar, A., Jain, S., Sudweeks, J., & Perez, M. (2023). 2 Driver Attention Modeling Through Evidence Accumulation and Gaze Fixation. In *Towards Human-Vehicle Harmonization* (pp. 13–28). De Gruyter. https://doi.org/10.1515/9783110981223-002

Savino, G., Pierini, M., Rizzi, M., & Frampton, R. (2013). Evaluation of an Autonomous Braking System in Real-World PTW Crashes. *Traffic Injury Prevention*, *14*(5), 532–543. https://doi.org/10.1080/15389588.2012.725878

Sevarin, A., Sebastian, W., Rößer, J., Mikschofsky, N., Menato, L., Hammer, T., Schneider, N., & Mark, C. (2020). Assessment of visual and haptic HMI concepts for hazard warning of powered two-wheeler riders. *Proceedings of the 13th International Motorcycle Conference, Cologne. 2020.*

Song, M., McLaughlin, S., & Doerzaph, Z. (2017). An on-road evaluation of connected motorcycle crash warning interface with different motorcycle types. *Transportation Research Part C: Emerging Technologies*, *74*, 34–50. https://doi.org/10.1016/j.trc.2016.11.005

Stephens, A. N., Brown, J., de Rome, L., Baldock, M. R. J., Fernandes, R., & Fitzharris, M. (2017). The relationship between Motorcycle Rider Behaviour Questionnaire scores and crashes for riders in Australia. *Accident Analysis & Prevention*, *102*, 202–212. https://doi.org/10.1016/j.aap.2017.03.007

Stewart, T. (2023). *Overview of motor vehicle traffic crashes in 2021*. (No. DOT HS 813 435). United States. Department of Transportation. National Highway Traffic Safety Administration.

Tak, S., Kim, S., & Yeo, H. (2015). Development of a Deceleration-Based Surrogate Safety Measure for Rear-End Collision Risk. *IEEE Transactions on Intelligent Transportation Systems*, *16*(5), 2435–2445. https://doi.org/10.1109/TITS.2015.2409374

Teoh, E. R., & Campbell, M. (2010). Role of motorcycle type in fatal motorcycle crashes. *Journal of Safety Research*, *41*(6), 507–512. https://doi.org/10.1016/j.jsr.2010.10.005

Terranova, P., Dean, M. E., Lucci, C., Piantini, S., Allen, T. J., Savino, G., & Gabler, H. C. (2022). Applicability Assessment of Active Safety Systems for Motorcycles Using Population-Based Crash Data: Cross-Country Comparison among Australia, Italy, and USA. *Sustainability*, *14*(13), 7563. https://doi.org/10.3390/su14137563

Terranova, P., Guo, F., & Perez, M. A. (2025). Evaluating risk factors associated with fatalities among powered two-wheeler crashes in the United States. *Traffic Injury Prevention*, 1–8. https://doi.org/10.1080/15389588.2025.2494235

Terranova, P., Liu, S.-Y., Jain, S., Engström, J., & Perez, M. A. (2024). Kinematic characterization of micro-mobility vehicles during evasive maneuvers. *Journal of Safety Research*, *91*, 342–353. https://doi.org/10.1016/j.jsr.2024.09.020

Terranova, P., & Perez, M. (2023). Developing a motorcycle injury risk model for planar collisions: Insights from the Motorcycle Crash Causation Study. *Accident Analysis and Prevention*, *193*. https://doi.org/10.1016/j.aap.2023.107292

Touliou, K., Margaritis, D., Spanidis, P., Nikolaou, S., & Bekiaris, E. (2012). Evaluation of Rider's Support Systems in Power Two Wheelers (PTWs). *Procedia - Social and Behavioral Sciences*, *48*, 632–641. https://doi.org/10.1016/j.sbspro.2012.06.1041

Valente, J. T., Jain, S., Amin, A., & Perez, M. A. (2023). Evaluation of the effectiveness of non-contact respiration rate detection for post-crash care application. *Accident Analysis & Prevention*, *193*, 107302. https://doi.org/10.1016/j.aap.2023.107302

Valente, J. T., Terranova, P., & Perez, M. A. (2024). *Creating a Dataset of Naturalistic Ambulance Driving: A Pilot Study of Two Ambulances*. Virginia Tech Transportation Institute. https://hdl.handle.net/10919/120842

Vlahogianni, E. I., Yannis, G., & Golias, J. C. (2014). Detecting Powered-Two-Wheeler incidents from high resolution naturalistic data. *Transportation Research Part F: Traffic Psychology and Behaviour*, *22*, 86–95. https://doi.org/10.1016/j.trf.2013.11.002

Vlahogianni, E. I., Yannis, G., Golias, J. C., Eliou, N., & Lemonakis, P. (2011). Identifying Riding Profiles Parameters from High Resolution Naturalistic Riding Data. *3rd International Conference on Road Safety and Simulation*.

Weare, A., Reed, N., Baldanzini, N., Prabhakar, A., Golias, J., Yannis, G., Vlahogianni, E., Spyropoulou, I., Val, C., Krishnakumar, R., & Martìnez, A. M. (2011). *Naturalistic Riding Study: Data Collection & Analysis.*

Williams V., McLaughlin, Fritz, S., McCall R., Rainey (in press). *Virginia Tech Transportation Institute Instrumented On-road Study of Motorcycle Riders Volume 1: Overview* (DOT # pending). National Highway Traffic Safety Administration.

Williams, V., McLaughlin, S. B., Williams, S. L., & Buche, T. (2015). Exploratory Analysis of Motorcycle Incidents Using Naturalistic Riding Data. *Transportation Research Record:*

Journal of the Transportation Research Board, *2520*(1), 151–156. https://doi.org/10.3141/2520-17

Williams, V., McLaughlin, S., Atwood, J., & Buche, T. (2016). Factors that Increase and Decrease Motorcyclist Crash Risk. In *Motorcycle Safety Foundation, Virginia*.

Williams, V., McLaughlin, S., Fritz, S., McCall R., & Rainey, C. (n.d.). *Instrumented On-road Study of Motorcycle Riders Volume 1: Overview*.

Williams, V., McLaughlin, S., McCall, R., & Buche, T. (2017). Motorcyclists' self-reported riding mileage versus actual riding mileage in the following year. *Journal of Safety Research*, *63*, 121–126. https://doi.org/10.1016/j.jsr.2017.10.004

Williams, V., McLaughlin, S., & Williams, S. (2013). An Exploratory Analysis of Motorcyclist Apparel Using Naturalistic Riding Data. In *Presentation*.

Williams, V., Rainey, C., Ali, G., McLaughlin, S., & Buche, T. (2018). Comparing Critical Event Deceleration for Motorcyclists and Drivers. *IFZ - International Motorcycle Conference*.

Yuen, C. W., Karim, M. R., & Saifizul, A. (2014). Investigation on Motorcyclist Riding Behaviour at Curve Entry Using Instrumented Motorcycle. *The Scientific World Journal*, *2014*, 1–9. https://doi.org/10.1155/2014/968946

Noonan, T. Z., Gershon, P., Domeyer, J., Mehler, B., & Reimer, B. (2023). Kinematic cues in driver-pedestrian communication to support safe road crossing. *Accident Analysis & Prevention, 192*, 107236.